



January 31, 2018

Docket No. 52-048

U.S. Nuclear Regulatory Commission
ATTN: Document Control Desk
One White Flint North
11555 Rockville Pike
Rockville, MD 20852-2738

SUBJECT: NuScale Power, LLC Response to NRC Request for Additional Information No. 133 (eRAI No. 8936) on the NuScale Design Certification Application

REFERENCES: 1. U.S. Nuclear Regulatory Commission, "Request for Additional Information No. 133 (eRAI No. 8936)," dated August 05, 2017
2. NuScale Power, LLC Response to NRC Request for Additional Information No. 133 (eRAI No. 8936) on the NuScale Design Certification Application, dated August 30, 2017 (ML17242A281)
3. NuScale Power, LLC Response to NRC Request for Additional Information No. 133 (eRAI No. 8936) on the NuScale Design Certification Application, dated October 03, 2017 (ML17276B886)

The purpose of this letter is to provide the NuScale Power, LLC (NuScale) response to the referenced NRC Request for Additional Information (RAI).

The Enclosure to this letter contains NuScale's response to the following RAI Question from NRC eRAI No. 8936:

- 03.07.02-7

The response to RAI Question 03.07.02-12 was previously provided in Reference 2. The response to RAI Questions 03.07.02-8, 03.07.02-9 and 03.07.02-11 were previously provided in Reference 3. The response to question 03.07.02-10 will be provided by April 20, 2018.

This letter and the enclosed response make no new regulatory commitments and no revisions to any existing regulatory commitments.

If you have any questions on this response, please contact Marty Bryan at 541-452-7172 or at mbryan@nucscalepower.com.

Sincerely,

A handwritten signature in black ink, appearing to read 'Zackary W. Rad', written over a horizontal line.

Zackary W. Rad
Director, Regulatory Affairs
NuScale Power, LLC



RAIO-0118-58472

Distribution: Gregory Cranston, NRC, OWFN-8G9A
Samuel Lee, NRC, OWFN-8G9A
Marieliz Vera, NRC, OWFN-8G9A

Enclosure 1: NuScale Response to NRC Request for Additional Information eRAI No. 8936



Enclosure 1:

NuScale Response to NRC Request for Additional Information eRAI No. 8936

Response to Request for Additional Information Docket No. 52-048

eRAI No.: 8936

Date of RAI Issue: 08/05/2017

NRC Question No.: 03.07.02-7

10 CFR 50 Appendix S requires that the safety functions of structures, systems, and components (SSCs) must be assured during and after the vibratory ground motion associated with the Safe Shutdown Earthquake (SSE) through design, testing, or qualification methods.

In FSAR Section 3.7.5, the applicant provided a brief description of the computer programs used in the analysis and design of the site-independent seismic Category I and Category II structures. However, it did not provide sufficient information regarding the verification & validation (V&V) of these programs. The applicant is requested to provide in the DCA information summarizing the V&V of the computer programs used to determine design-basis seismic demands for NuScale seismic Category I and II structures. The demonstration should test those characteristics of the software that mimic the physical conditions, material properties, and physical processes that represent the NuScale design in numerical analysis. The V&V should cover the full range of parameters used in NuScale design-basis seismic demand calculations including the discretization and aspect ratio of finite elements, Poisson's ratio, frequencies of analysis, and other parameters pertinent to seismic system analyses.

NuScale Response:

A summary report of the verification and validation (V&V) of the computer programs, used in the analysis and design of the NuScale Category I and Category II structures, is described in this response.

ANSYS is a commercial, general use finite element analysis (FEA) software. ANSYS is used to determine demand loads and stresses in structures, supports, equipment and components/assemblies. ANSYS Mechanical software offers a comprehensive product solution for structural linear, nonlinear, and dynamic analysis. The product provides a complete set of element behavior, material models, and equation solvers for a wide range of engineering problems. Table 1 summarizes all ANSYS verification problems for elements used in the NuScale models.



SAP2000 is a general-purpose, three-dimensional static and dynamic finite-element computer program. Analyses, up to and including calculation of deflections, forces, and stresses, may be done on structures constructed of any material or combination of materials.

It features a powerful graphical interface which is used to create/modify finite element models. This same interface is used to execute the analysis and for checking the optimization of the design. Graphical displays of the results, including real-time animations of time-history displacements are produced. SAP2000 provides automated generation of loads for design based on a number of National Standards.

The software can perform the following types of analyses: static linear analysis, static nonlinear analysis, modal analysis, dynamic response spectrum analysis, dynamic linear and nonlinear time history analysis, bridge analysis, moving load analysis, and buckling analysis. Tables 2 through 7 summarize all of the SAP2000 verification problems. The problems are categorized into groups based on the structural elements used or design type of the example.

SASSI, a System for Analysis of Soil-Structure Interaction, consists of a number of interrelated computer program modules which can be used to solve a wide range of dynamic soil-structure interaction (SSI) problems in two or three dimensions.

The verification problems for SASSI2010 are shown in Tables 8 through 16. The SASSI2010 V&V includes 30 test cases developed from nine different problems to verify the capabilities of SASSI2010. These test cases were developed using published literature and/or hand calculations. The problems are designed to check the program's capabilities under various conditions, in addition to showing accurate performance of the SASSI2010 methodologies. These problems provide reasonable assurance that a certified user (i.e., qualified engineer who possesses an understanding of soil-structure interaction) can apply SASSI2010 over the intended range of use. Other than the nine verification problems, an additional problem, Problem No. 10, was used to verify the overall validity of the SASSI2010 program to calculate correct static and dynamic responses for complex structures by comparing the results from SASSI2010 with the results from the independently verified SAP2000 program. Table 17 shows the descriptions and verification results of two analysis cases for Problem 10. In each case, the SASSI2010 program calculates the static and dynamic responses of a surface-founded, fixed-base complex structure. The total static reactions and the structural frequencies calculated by SASSI2010 are compared with the corresponding reactions and frequencies calculated by the verified SAP2000

The computer program SHAKE2000 computes the free-field response of a semi-infinite, horizontally layered soil column overlying a uniform half-space subjected to an input motion prescribed as the object motion in the form of vertically propagating shear waves. SHAKE2000 is used for the analysis of site-specific response and for the evaluation of earthquake effects on soil deposits. It provides an approximation of the dynamic response of a site. SHAKE2000 computes the response in a system of homogeneous, viscoelastic layers of infinite horizontal extent subjected to vertically traveling shear waves. Verification problems, summarized in Table



18, were designed to test SHAKE2000 major analytical capabilities.

The RspMatchEDT Module for SHAKE2000 is a pre- and post-processor for the RspMatch2009 program, which is part of SHAKE2000. The RspMatch2009 program performs a time-domain modification of an acceleration time history to make it compatible with a user-specified target spectrum. Table 19 provides a description of the RspMatch verification problems.

This software V&V summary tests those characteristics of the software that mimic the physical conditions, material properties, and physical processes that represent the NuScale design in numerical analysis. It also covers the full range of parameters used in NuScale design-basis, seismic demand calculations, including the discretization and aspect ratio of finite elements, Poisson's ratio, frequencies of analysis, and other parameters pertinent to seismic system analyses.

FSAR Tier 2, Section 3.7.5 is revised to include the above information.

Table 1: ANSYS Verification Problems

Problem No.	Problem Title	ANSYS Verification Problem Description	Method of Independent Verification
vm2	Beam Stresses and Deflections Beam188	A standard 30" WF beam, with cross-sectional area A , is supported and loaded on the overhangs by a uniformly distributed load w . Determine the maximum bending stress σ in the middle portion of the beam and the deflection δ at the middle of the beam.	S. Timoshenko, <i>Strength of Material, Part I, Elementary Theory and Problems</i> , 3rd Edition, D. Van Nostrand Co., Inc., New York, NY, 1955, p. 98, problem 4.
vm6	Pinched Cylinder Shell181	A thin-walled cylinder is pinched by force F at the middle of the cylinder length. Determine the radial displacement δ at the point where F is applied. The ends of the cylinder are free edges.	R. D. Cook, <i>Concepts and Applications of Finite Element Analysis</i> , 2nd Edition, John Wiley and Sons, Inc., New York, NY, 1981, pp. 284-287.
vm7	Plastic Compression of a Pipe Assembly Shell181	Two coaxial tubes, the inner one of 1020 CR steel and cross-sectional area A_s , and the outer one of 2024-T4 aluminum alloy and of area A_a , are compressed between heavy, flat end plates. Determine the load-deflection curve of the assembly as it is compressed into the plastic region by an axial displacement. Assume that the end plates are so stiff that both tubes are shortened by exactly the same amount.	H. Takemoto, R. D. Cook, "Some Modifications of an Isoparametric Shell Element", <i>International Journal for Numerical Methods in Engineering</i> , Vol. 7 No. 3, 1973.
vm9	Large Lateral Deflection of Unequal Stiffness Springs Combin14 Combin40	A two-spring system is subjected to a force F . Determine the strain energy of the system and the displacements δ_x and δ_y .	G. N. Vanderplaats, <i>Numerical Optimization Techniques for Engineering Design with Applications</i> , McGraw-Hill Book Co., Inc., New York, NY, 1984, pp. 72-73, ex. 3-1.
vm10	Bending of a Tee-Shaped Beam Beam188	Find the maximum tensile and compressive bending stresses in an unsymmetrical T beam subjected to uniform bending M_z , with dimensions and geometric properties.	S. H. Crandall, N. C. Dahl, <i>An Introduction to the Mechanics of Solids</i> , McGraw-Hill Book Co., Inc., New York, NY, 1959, pg. 294, ex. 7.2.

vm17	Snap-Through Buckling of a Hinged Shell63 Shell181 Shell281	A hinged cylindrical shell is subjected to a vertical point load (P) at its center. Find the vertical displacement (UY) at points A and B for the load of 1000 N.	C. C. Chang, "Periodically Restarted Quasi-Newton Updates in Constant Arc-Length Method", <i>Computers and Structures</i> , Vol. 41 No. 5, 1991, pp. 963-972.
vm19	Random Vibration Analysis of a Deep Simply-Supported Beam Beam188	A deep, simply-supported square beam of length l, thickness t, and mass density m, is subjected to random uniform force power spectral density. Determine the peak response PSD value.	NAFEMS, <i>Selected Benchmarks for Forced Vibration</i> , Report prepared by W. S. Atkins Engineering Sciences, April 1989, Test 5R.
vm21	Tie Rod with Lateral Loading Beam188	A tie rod is subjected to the action of a tensile force F and a uniform lateral load p. Determine the maximum deflection z_{max} , the slope Θ at the left-hand end, and the maximum bending moment M_{max} . In addition, determine the same three quantities for the unstiffened tie rod ($F = 0$).	S. Timoshenko, <i>Strength of Material, Part II, Elementary Theory and Problems</i> , 3rd Edition, D. Van Nostrand Co., Inc., New York, NY, 1956, pg. 42, article 6.
vm26	Large Deflection of a Cantilever SHELL181	A cantilevered plate of length l, width b, and thickness t is fixed at one end and subjected to a pure bending moment M at the free end. Determine the true (large deflection) free-end displacements and rotation, and the top surface stress at the fixed end, using shell elements.	K. J. Bathe, E. N. Dvorkin, "A Formulation of General Shell Elements - The Use of Mixed Interpolation of Tensorial Components", <i>Int. Journal for Numerical Methods in Engineering</i> , Vol. 22 No. 3, 1986, pg. 720.
vm27	Thermal Expansion to Close a Gap LINK180 CONTA178	An aluminum-alloy bar is fixed at one end and has a gap δ between its other end and a rigid wall when at ambient temperature T_a . Calculate the stress σ , and the thermal strain $\epsilon_{Thermal}$ in the bar after it has been heated to temperature T.	C. O. Harris, <i>Introduction to Stress Analysis</i> , The Macmillan Co., New York, NY, 1959, pg. 58, problem 8.
vm34	Bending of a Tapered Plate (Beam) SHELL63 BEAM188 SHELL181 SHELL281	A tapered cantilever plate of rectangular cross-section is subjected to a load F at its tip. Find the maximum deflection δ and the maximum principal stress σ_1 in the plate.	C. O. Harris, <i>Introduction to Stress Analysis</i> , The Macmillan Co., New York, NY, 1959, pg. 114, problem 61.

vm36	Limit Moment Analysis Beam188 COMBIN40	A symmetric cross-section beam of bending stiffness EI_y , and height h , totally fixed at C, simply-supported at A, is subjected to a concentrated load P at point B. Verify that a load P which is slightly smaller than the theoretical load limit P_L will cause elastic deformation and that a load which is slightly larger than P_L will cause plastic deformation. Also determine the maximum deflection δ , the reaction force at the left end R_A , and the reaction moment at the right end M_C just prior to the development of a plastic hinge.	S. H. Crandall, N. C. Dahl, <i>An Introduction to the Mechanics of Solids</i> , McGraw-Hill Book Co., Inc., New York, NY, 1959, pg. 389, ex. 8.9.
vm37	Elongation of a Solid Bar Solid 145 Solid185 Solid45 SOLSH190	A tapered aluminum alloy bar of square cross-section and length L is suspended from a ceiling. An axial load F is applied to the free end of the bar. Determine the maximum axial deflection δ in the bar and the axial stress σ_y at mid-length ($Y = L/2$).	C. O. Harris, <i>Introduction to Stress Analysis</i> , The Macmillan Co., New York, NY, 1959, pg. 237, problem 4.
vm38	Internal Pressure Loading of a Thick-Walled Cylinder Plane182 Solid185 Surf153 Surf154	A long, thick-walled cylinder is subjected to an internal pressure p (with no end cap load). Determine the radial stress, σ_r , and the tangential (hoop) stress, σ_t , at locations near the inner and outer surfaces of the cylinder for a pressure, p_{el} , just below the yield strength of the material, a fully elastic material condition.	S. Timoshenko, <i>Strength of Material, Part II, Elementary Theory and Problems</i> , 3rd Edition, D. Van Nostrand Co., Inc., New York, NY, 1956, pg. 388, article 70.

vm39	Bending of a Circular Plate with a Center Hole Shell63 Shell181	A circular plate of thickness t with a center hole is rigidly attached along the inner edge and unsupported along the outer edge. The plate is subjected to bending by a moment M_a applied uniformly along the outer edge. Determine the maximum deflection δ and the maximum slope Φ of the plate. In addition, determine the moment M and stress σ_x at the top centroidal locations of element 1 (near inner edge) and element 6 (near outer edge).	S. Timoshenko, <i>Strength of Material, Part II, Elementary Theory and Problems</i> , 3rd Edition, D. Van Nostrand Co., Inc., New York, NY, 1956, pg. 111, eq. E and F.
vm40	Large Deflection and Rotation of a Beam Pinned at One End Beam188	A massless beam of length L is initially at position AB on a horizontal frictionless table. Point A is pinned to the table and given a large rotation Θ_z through a full revolution at speed ω_z . Determine the position of the beam in terms of δ , and Θ at various angular locations. Show that the beam has no axial stress σ at any position.	Any basic mathematics book
vm41	Small Deflection of a Rigid Beam <u>MATRIX27</u> <u>BEAM188</u>	A very stiff beam of length L , subjected to a lateral load F , is initially at position AB on a horizontal table. Point A is pinned to the table and restrained from rotation by a relatively weak torsion spring. Determine the final position of the beam in terms of δ_x , δ_y , and Θ . Show that the bending stress in the beam σ_{bend} is negligible.	Any basic Statics and Strength of Materials Book
vm42	Barrel Vault Roof Under Self Weight Shell181 Shell281	A cylindrical shell roof of density ρ is subjected to a loading of its own weight. The roof is supported by walls at each end and is free along the sides. Find the x and y displacements at point A and the top and bottom stresses at points A and B. Express stresses in the cylindrical coordinate system.	R. D. Cook, <i>Concepts and Applications of Finite Element Analysis</i> , 2nd Edition, John Wiley and Sons, Inc., New York, NY, 1981, pp. 284-287.

vm45	Natural Frequency of a Spring-Mass System Combin14 Mass21	An instrument of weight W is set on a rubber mount system having a stiffness k . Determine its natural frequency of vibration f .	W. T. Thomson, <i>Vibration Theory and Applications</i> , 2nd Printing, Prentice-Hall, Inc., Englewood Cliffs, NJ, 1965, pg. 6, ex. 1.2-2.
vm47	Torsional Frequency of a Suspended Disk Combin14 Mass21	A disk of mass m which has a polar moment of inertia J is suspended at the end of a slender wire. The torsional stiffness of the wire is k_θ . Determine the natural frequency f of the disk in torsion.	W. T. Thomson, <i>Vibration Theory and Applications</i> , 2nd Printing, Prentice-Hall, Inc., Englewood Cliffs, NJ, 1965, pg. 10, ex. 1.3-2
vm48	Natural Frequency of a Motor-Generator BEAM188 Mass21	A small generator of mass m is driven off a main engine through a solid steel shaft of diameter d . If the polar moment of inertia of the generator rotor is J , determine the natural frequency f in torsion. Assume that the engine is large compared to the rotor so that the engine end of the shaft may be assumed to be fixed. Neglect the mass of the shaft also.	W. T. Thomson, <i>Vibration Theory and Applications</i> , 2nd Printing, Prentice-Hall, Inc., Englewood Cliffs, NJ, 1965, pg. 10, ex. 1.3-3
vm51	Electrostatic Forces Between Charged Spheres <u>SOLID123</u> <u>SOLID122</u> <u>INFIN111</u> <u>PLANE121</u> <u>MESH200</u>	Two spheres with radii $= 1$ m, separated by a distance of 3 m, are subjected to a surface charge. Find the resultant electrostatic force between the spheres.	Any General Physics Textbook
vm52	Automobile Suspension System Vibration <u>BEAM188</u> <u>COMBIN14</u> <u>MASS21</u>	An automobile suspension system is simplified to consider only two major motions of the system: · up and down linear motion of the body · pitching angular motion of the body If the body is idealized as a lumped mass with weight W and radius of gyration r , determine the corresponding coupled frequencies f_1 and f_2 .	W. T. Thomson, <i>Vibration Theory and Applications</i> , 2nd Printing, Prentice-Hall, Inc., Englewood Cliffs, NJ, 1965, pg. 181, ex. 6.7-1

vm54	Vibration of a Rotating Cantilever Blade <u>SHELL63 SOLSH190 SHELL181 SHELL281</u>	A blade is cantilevered from a rigid rotating cylinder. Determine the fundamental frequency of vibration of the blade, f , when the cylinder is spinning at a rate of Ω .	W. Carnegie, "Vibrations of Rotating Cantilever Blading", <i>Journal Mechanical Engineering Science</i> , Vol. 1 No. 3, 1959, pg. 239
vm56	Hyperelastic Thick Cylinder Under Internal Pressure <u>PLANE183 SOLID185 SOLID186</u>	An infinitely long cylinder is made of Mooney-Rivlin type material. An internal pressure of P_i is applied. Find the radial displacement at the inner radius and the radial stress at radius $R = 8.16$ in (center of 1st element).	J. T. Oden, <i>Finite Elements of Nonlinear Continua</i> , McGraw-Hill Book Co., Inc., New York, NY, 1972, pp. 325-331.
vm57	Torsional Frequencies of a Drill Pipe <u>PIPE16 MASS21 PIPE288 PIPE289 BEAM188 BEAM189</u>	Determine the first two natural frequencies f_1 and f_2 of an oil-well drill pipe of length l and polar moment of inertia I_p fixed at the upper end and terminating at the lower end to a drill collar with torsional mass inertia J_o . The drill collar length is small compared to the pipe length.	W. T. Thomson, <i>Vibration Theory and Applications</i> , 2nd Printing, Prentice-Hall, Inc., Englewood Cliffs, NJ, 1965, pg. 272, ex. 8.4-5.
vm59	Lateral Vibration of an Axially-loaded Bar <u>BEAM188</u>	A square cross-sectioned bar of length l and weight per unit length γA is pinned at its ends and subjected to an axial compressive force F . Determine the stress σ and the axial displacement δ of the bar under these conditions. Determine the first three natural frequencies f_j of lateral vibration of the bar.	S. Timoshenko, D. H. Young, <i>Vibration Problems in Engineering</i> , 3rd Edition, D. Van Nostrand Co., Inc., New York, NY, 1955, pg. 374, article 59.
vm61	Longitudinal Vibration of a Free-free Rod <u>BEAM188</u>	Determine the first three natural frequencies f_j of a free-free rod (a rod with both ends free) having a length 800 in.	W. T. Thomson, <i>Vibration Theory and Applications</i> , 2nd Printing, Prentice-Hall, Inc., Englewood Cliffs, NJ, 1965, pg. 269, ex. 8.3-1.
vm62	Vibration of a Wedge <u>SHELL63 SHELL181 SHELL281</u>	Determine the fundamental frequency of out-of-plane vibration f of a wedge-shaped plate of uniform thickness t , base $2b$, and length 16in.	S. Timoshenko, D. H. Young, <i>Vibration Problems in Engineering</i> , 3rd Edition, D. Van Nostrand Co., Inc., New York, NY, 1955, pg. 392, article 62.

vm63	Static Hertz Contact Problem <u>PLANE82</u> <u>PLANE183</u> <u>CONTA178</u>	A sphere of radius r is pressed against a rigid flat plane. Determine the contact radius, a , for a given load F .	S. Timoshenko, J. N. Goodier, <i>Theory of Elasticity</i> , 3rd Edition, McGraw-Hill Book Co., Inc., New York, NY, 1970, pg. 409-413, article 140.
vm65	Transient Response of a Ball Impacting a Flexible Surface <u>MASS21</u> <u>CONTA175</u>	A rigid ball of mass m is dropped through a height h onto a flexible surface of stiffness k . Determine the velocity, kinetic energy, and displacement y of the ball at impact and the maximum displacement of the ball.	W. T. Thomson, <i>Vibration Theory and Applications</i> , 2nd Printing, Prentice-Hall, Inc., Englewood Cliffs, NJ, 1965, pg. 110, ex. 4.6-1.
vm66	Vibration of a Flat Plate <u>SHELL63</u> <u>SOLSH190</u> <u>SHELL181</u> <u>SHELL281</u>	Determine the fundamental natural frequency of lateral vibration f of a flat rectangular plate. The plate is of uniform thickness t , width $2b$, and length 16 in.	S. Timoshenko, D. H. Young, <i>Vibration Problems in Engineering</i> , 3rd Edition, D. Van Nostrand Co., Inc., New York, NY, 1955, pg. 338, article 53.
vm77	Transient Response to a Constant Force <u>BEAM188</u> <u>MASS21</u>	A steel beam of length and geometric properties is supporting a concentrated mass, m . The beam is subjected to a dynamic load $F(t)$ with a rise time t_r and a maximum value F_1 . If the weight of the beam is considered negligible, determine the time of maximum displacement response t_{max} and the maximum displacement response y_{max} . Additionally, determine the maximum bending stress σ_{bend} in the beam.	J. M. Biggs, <i>Introduction to Structural Dynamics</i> , McGraw-Hill Book Co., Inc., New York, NY, 1964, pg. 50, ex. E.
vm80	Plastic Response to a Suddenly Applied Constant Force <u>LINK180</u> <u>MASS21</u>	A mass m supported on a thin rod of area A and length 100 in is subjected to the action of a suddenly applied constant force F_1 . Determine the maximum deflection y_{max} and minimum deflection y_{min} of the mass, neglecting the mass of the rod.	J. M. Biggs, <i>Introduction to Structural Dynamics</i> , McGraw-Hill Book Co., Inc., New York, NY, 1964, pg. 69, article 2.7.

vm81	Transient Response of a Dropped Container <u>COMBIN40</u> <u>MASS21</u>	A mass m is packaged in a rigid box, and dropped through a height h . Determine the velocity and displacement y of the mass at impact and the maximum displacement of the mass. Assume that the mass of the box is large compared to that of the enclosed mass m and that the box remains in contact with the floor after impact	W. T. Thomson, <i>Vibration Theory and Applications</i> , 2nd Printing, Prentice-Hall, Inc., Englewood Cliffs, NJ, 1965, pg. 110, ex. 4.6-1.
vm82	Simply Supported Laminated Plate Under Pressure <u>SOLSH190</u> <u>SOLID186</u> <u>SHELL181</u> <u>SHELL281</u> <u>SOLID185</u>	A simply-supported, square, cross-ply laminated plate is subjected to a uniform pressure p_0 . The stacking sequence of the plies is symmetric about the middle plane. Determine the center deflection δ (Z-direction) of the plate due to the pressure load.	J. N. Reddy, "Exact Solutions of Moderately Thick Laminated Shells", <i>ASCE Journal Engineering Mechanics</i> , Vol. 110 No. 5, 1984, pp. 794-809.
vm89	Natural Frequencies of a Two-mass-spring System <u>COMBIN14</u> <u>MASS21</u>	Determine the normal modes and natural frequencies of the system for the values of the masses and spring stiffnesses given.	W. T. Thomson, <i>Vibration Theory and Applications</i> , 2nd Printing, Prentice-Hall, Inc., Englewood Cliffs, NJ, 1965, pg. 163, ex. 6.2-2.
vm90	Harmonic Response of a Two-Mass-Spring System <u>COMBIN14</u> <u>MASS21</u>	Determine the response amplitude (X_i) and phase angle (Φ_i) for each mass (m_i) when excited by a harmonic force ($F_1 \sin \omega t$) acting on mass m_1 .	W. T. Thomson, <i>Vibration Theory and Applications</i> , 2nd Printing, Prentice-Hall, Inc., Englewood Cliffs, NJ, 1965, pg. 178, ex. 6.6-1.
vm91	Large Rotation of a Swinging Pendulum <u>LINK180</u> <u>MASS21</u>	A pendulum consists of a mass m supported by a rod of length 100 in and cross-sectional area A . Determine the motion of the pendulum in terms of the displacement of the mass from its initial position Θ_0 in the x and y directions, δ_x and δ_y , respectively. The pendulum starts with zero initial velocity.	W. T. Thomson, <i>Vibration Theory and Applications</i> , 2nd Printing, Prentice-Hall, Inc., Englewood Cliffs, NJ, 1965, pg. 138, ex. 5.4-1.

vm127	Buckling of a Bar with Hinged Ends (Line Elements) <u>BEAM188</u>	Determine the critical buckling load of an axially loaded long slender bar of length 200in with hinged ends. The bar has a square cross-section with width and height set to 0.5 inches.	S. Timoshenko, <i>Strength of Material, Part II, Elementary Theory and Problems</i> , 3rd Edition, D. Van Nostrand Co., Inc., New York, NY, 1956, pg. 148, article 29.
vm131	Acceleration of a Rotating Crane Boom <u>MASS21</u>	Determine the acceleration at the tip P of a crane boom that has a constant angular velocity ω rotation (Ω) while being raised with a constant angular velocity (ω).	F. P. Beer, E. R. Johnston, Jr., <i>Vector Mechanics for Engineers, Statics and Dynamics</i> , 5th Edition, McGraw-Hill Book Co., Inc., New York, NY, 1962, pg. 616, problem 15.13.
vm133	Motion of a Rod Due to Irradiation Induced Creep <u>BEAM188</u>	A rod of length 1 in. and square cross-sectional area A is held at a constant stress σ_0 at a temperature T_0 . The rod is also subjected to a constant neutron flux Φ . The rod material has an irradiation-induced creep strain rate given by the relationship $d\epsilon_{cr} / dt = k_1 \sigma \Phi e^{- (\Phi t / k_2)}$. Determine the amount of creep strain ϵ_{cr} accumulated up to 5 hours.	Any basic calculus book
vm134	Plastic Bending of a Clamped I-Beam <u>BEAM188</u>	A wide-flanged I-beam of length 144in, with clamped ends, is uniformly loaded. Investigate the behavior of the beam at load w_1 when yielding just begins at the ends, at load w_2 , when the midpoint begins to yield, and at load w_3 , when pronounced plastic yielding has occurred.	N. J. Hoff, <i>The Analysis of Structures</i> , John Wiley and Sons, Inc., New York, NY, 1956, pg. 388, article 4.5.
vm136	Large Deflection of a Buckled Bar (the Elastica) <u>BEAM188</u>	A slender square cross-sectional bar of length l, and area A, fixed at the base and free at the upper end, is loaded with a value larger than the critical buckling load. Determine the displacement (ΔX , ΔY , Θ) of the free end and display the deformed shape of the bar at various loadings.	S. Timoshenko, J. M. Gere, <i>Theory of Elastic Stability</i> , 2nd Edition, McGraw-Hill Book Co. Inc., New York, NY, 1961, pg. 78, article 2.7.

vm141	Diametral Compression of a Disk <u>PLANE82</u> <u>PLANE183</u> <u>MATRIX50</u> <u>SHELL181</u> <u>SHELL281</u>	Two equal and opposite forces act along the vertical diameter of a disk. Determine the compressive stress at the center of the disk and on the major horizontal diameter at 0.1 in. from the center.	S. Timoshenko, J. N. Goodier, <i>Theory of Elasticity</i> , 2nd Edition, McGraw-Hill Book Co., Inc., New York, NY, 1951, pg. 107, article 37.
vm143	Fracture Mechanics Stress for a Crack in a Plate <u>SOLID95</u> <u>SOLID45</u> <u>PLANE183</u> <u>SOLID186</u> <u>SOLID185</u>	A long plate with a center crack is subjected to an end tensile stress σ_0 . Determine the fracture mechanics stress intensity factor K_I .	W. F. Brown, Jr., J. E. Srawley, "Plane Strain Crack Toughness Testing of High Strength Metallic Materials", <i>ASTM STP-410</i> , 1966.
vm144	Bending of a Composite Beam <u>SOLID185</u> <u>SOLID186</u> <u>SOLSH190</u> <u>SHELL281</u>	A beam of length l and width w , made up of two layers of different materials, is subjected to a uniform rise in temperature from T_{ref} to T_0 and a bending moment M_y at the free-end. Determine the free-end displacement δ (in the Z-direction) and the X-direction stresses at the top and bottom surfaces of the layered beam. E_i and α_i correspond to the Young's modulus and thermal coefficient of expansion for layer i , respectively.	R. J. Roark, W. C. Young, <i>Formulas for Stress and Strain</i> , McGraw-Hill Book Co., Inc., New York, NY, 1975, pg. 112-114, article 7.2.
vm145	Stretching of an Orthotropic Solid <u>SOLID185</u>	A unit cube of side 1 in, having orthotropic material properties, is subjected to forces F_x and F_y . Three orthogonal faces are supported and the opposite three faces are free. Determine the translational displacements (ΔX , ΔY , and ΔZ) of the free faces.	S. H. Crandall, N. C. Dahl, <i>An Introduction to the Mechanics of Solids</i> , McGraw-Hill Book Co., Inc., New York, NY, 1959, pg. 225.

vm149	Residual Vector in Mode-Superposition Harmonic Analysis <u>COMBIN14</u> <u>MASS21</u>	A mode-superposition harmonic analysis is performed on a spring-mass model for two cases: Case 1: Extracting all available modes Case 2: Extracting one mode and residual vector (<u>RESVEC</u>)	J.M.Dickens, J.M. Nakagawa, M.J. Wittbrodt, "A Critique of Mode Acceleration and Modal Truncation Augmentation Methods for Modal Response Analysis". <i>Computers & Structures</i> , Vol.62, pp.985-998, 1997.
vm150 From Version 14	Acceleration of a Tank of Fluid <u>FLUID80</u>	A large rectangular tank is partially filled with an incompressible liquid. The tank has a constant acceleration a to the right. Determine the elevation of the liquid surface relative to the zero acceleration elevation along the Y-axis. Also determine the slope of the free surface and the pressure p in the fluid near the bottom left corner of the tank.	K. Brenkert, Jr., <i>Elementary Theoretical Fluid Mechanics</i> , John Wiley and Sons, Inc., New York, NY, 1960, pg. 50, article 17.
vm153	3-D Non-axisymmetric Vibration of a Stretched Membrane <u>SHELL181</u>	A circular membrane under a uniform tension S is allowed to vibrate freely. The edge of the membrane is simply supported. Determine the natural frequencies $f_{i,j}$ for the first two modes of vibration ($j = 1, 2 = \text{no. of nodal circles, including the boundary}$) for the first two harmonics ($i = 0, 1 = \text{no. of harmonic indices}$).	S. Timoshenko, D. H. Young, <i>Vibration Problems in Engineering</i> , 3rd Edition, D. Van Nostrand Co., Inc., New York, NY, 1955, pg. 439, article 69.
vm154	Vibration of a Fluid Coupling <u>FLUID38</u> <u>COMBIN14</u>	A long cylinder is immersed in a circular hole. The cylinder is separated from the containment surface by a frictionless, incompressible liquid annulus. A spring restraint is attached to the cylinder from ground. Determine the natural frequency f of the system based upon the hydrodynamic mass of the liquid annulus.	R. J. Fritz, "The Effect of Liquids on the Dynamic Motions of Immersed Solids", <i>ASME, J. of Engr. for Industry</i> , Vol. 94, Feb. 1972, pp. 167-173.

vm156	Natural Frequency of a Nonlinear Spring-Mass System <u>COMBIN39</u> <u>MASS21</u>	A mass is supported from a spring having nonlinear characteristics. The mass is displaced an amount δ from its equilibrium position and released (with no initial velocity). Find the corresponding period of vibration τ .	S. Timoshenko, D. H. Young, <i>Vibration Problems in Engineering</i> , 3rd Edition, D. Van Nostrand Co., Inc., New York, NY, 1955, pg. 141.
vm171	Permanent Magnet Circuit With an Elastic Keeper <u>PLANE13</u> <u>COMBIN14</u>	A permanent magnet circuit consisting of a highly-permeable core and a permanent magnet is used to model a relay switch. An elastic keeper is modeled with a highly permeable iron and two springs. Assuming no flux leakage, determine the equilibrium displacements, δ , of the keeper and the operating point (flux density) in the permanent magnet.	F. C. Moon, <i>Magneto-Solid Mechanics</i> , John Wiley and Sons, Inc., New York, NY, 1984, pg. 275.
vm177	Natural Frequency of a Submerged Ring <u>FLUID30</u> <u>SHELL63</u> <u>FLUID29</u> <u>BEAM188</u> <u>SHELL181</u> <u>SHELL281</u> <u>FLUID221</u>	A steel ring is submerged in a compressible fluid (water). Determine the lowest natural frequency for x-y plane bending modes of the fluid-structure system.	E. A. Schroeder, M. S. Marcus, "Finite Element Solution of Fluid Structure Interaction Problems", Shock and Vibration Symposium, San Diego, CA, 1975.
vm179	Dynamic Double Rotation of a Jointed Beam <u>MPC184</u> <u>MASS21</u> <u>BEAM188</u>	A torque M_1 is applied at the pinned end of an aluminum beam to cause a 90° rotation. A second torque M_2 is then applied at a revolute joint in the beam to create an out-of-plane rotation. The joint has a rotational stiffness k , inertial mass J , frictional torque T_f , and locks when a 5° rotation occurs. Structural mass elements with rotational mass are added at the joint nodes. Determine the position of the beam at the end of each rotation.	Any basic mechanics text

vm180	Bending of a Curved Beam <u>PLANE183</u> <u>BEAM188</u>	A curved beam spans a 90° arc. The bottom end is supported while the top end is free. For a bending moment M applied at the top end, determine the maximum tensile stress σ_t and the maximum compressive stress σ_c in the beam.	S. Timoshenko, J. N. Goodier, <i>Theory of Elasticity</i> , 3rd Edition, McGraw-Hill Book Co. Inc., New York, NY, 1970, pg. 73, article 29.
vm189	Stress Relaxation of a Chloroprene Rubber <u>SOLID185</u>	A uniaxial compression test with intermittent relaxation time is performed on a block modeled with Chloroprene rubber. The block is subjected to true strain rates of $\dot{\epsilon} = -0.002s^{-1}$ and $\dot{\epsilon} = -0.1s^{-1}$ with 120s relaxation time at $\dot{\epsilon} = -0.3$ and $\dot{\epsilon} = -0.6$, respectively.	Dal, H. et al. "Bergstrom-Boyce model for nonlinear finite rubber viscoelasticity: theoretical aspects and algorithmic treatment for the FE method". <i>Computational Mechanics</i> . 2009, 44: 809-823
vm191	Hertz Contact Between Two Cylinders <u>CONTA175</u> <u>PLANE182</u> <u>SOLID185</u>	Two long cylinders of radii R_1 and R_2 , in frictionless contact with their axes parallel to each other are pressed together with a force per unit length, F . Determine the semi-contact length b and the approach distance d .	N. Chandrasekaran, W. E. Haisler, R. E. Goforth, "Finite Element Analysis of Hertz Contact Problem with Friction", <i>Finite Elements in Analysis and Design</i> , Vol. 3, 1987, pp. 39-56.
vm195	Toggle Mechanism <u>MPC184</u> <u>BEAM188</u> <u>COMBIN14</u> <u>LINK11</u>	Determine the maximum force (F_{max}) of a toggle mechanism acting upon a resisting spring.	G. H. Martin, <i>Kinematics and Dynamics of Machines</i> , 2nd Edition, McGraw-Hill Book Co., Inc., New York, NY, 1982, pp. 55-56, fig. 3-22.
vm196	Counter-Balanced Loads on a Block <u>SOLID45</u> <u>SOLID185</u> <u>MATRIX50</u>	Determine the free-body moments (M_x , M_y , M_z) about the origin and the rotational accelerations (ω_x , ω_y , ω_z) at the center of mass of an aluminum block due to the forces F_x and F_y .	Any basic mechanics text
vm198	Large Strain In-plane Torsion Test <u>PLANE182</u> <u>PLANE183</u> <u>SOLID185</u>	A hollow, thick-walled, long cylinder made of an elastoplastic material is under an in-plane torsional loading which causes the inner surface of the cylinder to undergo a rotation of 60°. Find the maximum shear stress (τ_{max}) developed at the inner surface at the end of loading.	J. C. Nagtegaal, J. E. DeJong, "Some Computational Aspects of Elastic-Plastic Strain Analysis", <i>Intl J. of Numerical Methods in Engineering</i> , Vol. 17, 1981, pp. 15-41.

vm199	Viscoplastic Analysis of a Body (Shear Deformation) <u>PLANE182</u> <u>PLANE183</u> <u>SOLID185</u>	A cubic shaped body made up of a viscoplastic material obeying Anand's law undergoes uniaxial shear deformation at a constant rate of 0.01 cm/s. The temperature of the body is maintained at 400°C. Find the shear load (F_x) required to maintain the deformation rate of 0.01 cm/sec at time equal to 20 seconds.	B. Lwo, G. M. Eggert, "An Implicit Stress Update Algorithm Using a Plastic Predictor", Submitted to Computer Methods in Applied Mechanics and Engineering, January 1991.
vm201	Rubber Cylinder Pressed Between Two Plates <u>PLANE182</u> <u>SOLID185</u> <u>TARGE169</u> <u>TARGE170</u> <u>CONTA175</u> <u>MESH200</u>	A long rubber cylinder is pressed between two rigid plates using a maximum imposed displacement of δ_{max} . Determine the force-deflection response.	T. Tussman, K-J Bathe, "A Finite Element Formulation for Nonlinear Incompressible Elastic and Inelastic Analysis", <i>Computers and Structures</i> , Vol. 26 Nos 1/2, 1987, pp. 357-409.
vm211	Rubber Cylinder Pressed Between Two Plates <u>PLANE182</u> <u>PLANE183</u> <u>SOLID185</u> <u>CONTA171</u> <u>CONTA172</u> <u>CONTA173</u> <u>CONTA174</u> <u>TARGE169</u> <u>TARGE170</u>	A long rubber cylinder is pressed between two rigid plates using a maximum imposed displacement of δ_{max} . Determine the force-deflection response.	T. Tussman, K-J Bathe, "A Finite Element Formulation for Nonlinear Incompressible Elastic and Inelastic Analysis", <i>Computers and Structures</i> , Vol. 26 Nos 1/2, 1987, pp. 357-409.

vm212	DDAM Analysis of Foundation System (2-DOF System) <u>MASS21</u> <u>COMBIN40</u> <u>BEAM188</u>	A simple equipment-foundation system is modeled using a spring-damper element (<u>COMBIN40</u>) representing the foundation, a beam element (<u>BEAM188</u>) representing the equipment, and a mass element (<u>MASS21</u>) representing the equipment mass. Shock loading is applied at the fixed base of the foundation system along the athwart ship direction. The shock spectrum is based on the ship type, mounting location, direction of shock, and type of design (elastic or elastic-plastic). DDAM analysis is performed on this system to determine natural frequency, deflection, and shock design value.	O'Hara, G.J., Cunniff, P. F., "Interim Design Values for Shock Design of Shipboard Equipment", <i>NRL Memorandum Report 1396</i> , 1963, p. 10.
vm216	Lateral Buckling of a Right Angle Frame <u>BEAM188</u> <u>BEAM189</u>	A 0.6in thick plate that is 30in wide is fashioned into a cantilever right angle frame, and is subjected to an in-plane fixed end load (F_x). The frame is driven to buckling mode by a perturbation load (F_z) applied at the free end, normal to the plane of the frame. This perturbation is removed close to the buckling load. Determine the critical load.	J. C. Simo, L. Vu-Quoc, "Three-Dimensional Finite-Strain Rod Model, Part II", <i>Computer Methods in Applied Mechanical Engineering</i> , Vol. 58, 1986, pp. 79-116.
vm217	Portal Frame Under Symmetric Loading <u>BEAM188</u> <u>BEAM189</u>	A rigid rectangular frame is subjected to a uniform distributed load w across the span. Determine the maximum rotation, and maximum bending moment. The moment of inertia for the span, I_{span} is five times the moment of inertia for the columns, I_{col} .	N. J. Hoff, <i>The Analysis of Structures</i> , John Wiley and Sons, Inc., New York, NY, 1956, pp. 115-119.
vm218	Hyperelastic Circular Plate <u>SHELL181</u> <u>SHELL208</u> <u>SHELL209</u> <u>SHELL281</u>	A flat, circular membrane made of a rubber material is subjected to uniform water pressure. The edges of the membrane are fixed. Determine the response as pressure is increased to 50 psi.	J. T. Oden, <i>Finite Elements of Nonlinear Continua</i> , McGraw-Hill Book Co., Inc., New York, NY, 1972, pp. 318-321.

vm219	Frequency Response of a Prestressed Beam using APDL MATH Commands <u>BEAM188</u> <u>TRANS126</u>	A beam is in series with an electromechanical transducer. With a voltage applied to the beam, determine the prestressed natural frequencies of the beam.	R. D. Blevins, Formulas for Natural Frequency and Mode Shape, Van Nostrand Reinhold Co., pg. 144, equation 8-20.
vm221	Simulation of Shape Memory Alloy Effect <u>SOLID185</u>	A block is composed of shape memory alloy material. The block, which has an initial temperature of 253.15K, is loaded up to 70 MPA to obtain detwinned martensitic structure, and then unloaded until it is stress free to obtain a martensitic structure in which residual strain remains. The temperature is then increased to 259.15K to recover residual strain and regain the austenitic structure. The final stress and strain is obtained and compared against the reference solution.	A. Souza, et al. "Three-dimensional model for solids undergoing stress-induced phase transformation". <i>Eur. J. Mech. A/Solids</i> . 1998, 17: 789-806.
vm222	Warping Torsion Bar <u>BEAM188</u> <u>BEAM189</u>	A cantilever I-beam is fixed at both ends and a uniform moment, M_x , is applied along its length	C-N Chen, "The Warping Torsion Bar Model of the Differential Quadrature Method", <i>Computers and Structures</i> , Vol. 66 No. 2-3, 1998, pp. 249-257.
vm225	Rectangular Cross-Section Bar with Preload <u>SOLID185</u> <u>PRETS179</u> <u>SOLID186</u>	A compressive preload is applied to a rectangular cross-section bar. Determine the resulting stress and displacement.	Engineering Statics Text
vm232	Stress Intensity Factor for a Single Edge Crack with Pressure Load Using UMM Method <u>SOLID185</u> <u>SOLID186</u> <u>SOLID187</u>	A solid block with width $W = 1$ m, height $H = 5$ m, and thickness $t = 0.1$ m is modeled with a single edge crack of length $a = 0.1$ m. The crack is subjected to a pressure load P and the stress intensity factor is determined using the UMM method (CINT , UMM, ON). The results are compared to the analytical solution given in the reference (point b in Table 6.1, p. 130).	Stephens, R.I., Fatemi, A., Stephens, R.R., Fuchs, H.O., <i>Metal Fatigue in Engineering</i> , 2nd Edition, 2006, pg. 130.

vm234	Cyclic Loading of a Rubber Block <u>SOLID185</u>	A cube of rubber is subjected to a sinusoidal displacement controlled load with a mean value of zero (completely reversed). The load amplitude is constant within a full cycle (4 seconds) and increases with each successive cycle. For the first period $A = 0.01$ and it increases by 0.01 each cycle until the fourth when $A = 0.04$. At $t = 16$ seconds the load is removed and the residual stresses are permitted to relax.	G. A. Holzapfel, "On Large Strain Viscoelasticity: Continuum Formulation and Finite Element Applications to Elastomeric Structures", <i>International Journal for Numerical Methods in Engineering</i> , Vol. 39, 1996, pp. 3903-3926.
vm235	Frequency Response of a Prestressed Beam <u>BEAM188</u> <u>TRANS126</u>	A beam is in series with an electromechanical transducer. With a voltage applied to the beam, determine the prestressed natural frequencies of the beam.	R. D. Blevins, <i>Formulas for Natural Frequency and Mode Shape</i> , Van Nostrand Reinhold Co., pg. 144, equation 8-20.
vm236	Hysteresis Calculation of a Beam Under Electrostatic Load <u>PLANE223</u> <u>PLANE182</u> <u>CONTA178</u>	A beam of length $L = 80 \mu\text{m}$ at a height $T = 0.5 \mu\text{m}$ is suspended $0.7 \mu\text{m}$ above a ground plane and is clamped at either end. Using this beam, model the hysteresis (pull-in and release behaviors) when it is placed under electrostatic load.	J. R. Gilbert, G. K. Ananthasuresh, S. D. Senturia, "3D Modeling of Contact Problems and Hysteresis in Coupled Electro-Mechanics", <i>MEMS</i> , 1996, pp. 127-132.
vm239	Mechanics of the Revolute and Universal Joints <u>BEAM188</u> <u>MPC184</u> <u>TARGE170</u>	A double universal joint drive shaft drives a simple slider-crank mechanism. Compare the rotations at different points in the drive shaft with the applied rotation. Also, show the linear motion caused by the slider-crank satisfied the appropriate equation.	J. E. Shigley, J. J. Uicker, Jr., <i>Theory of Machines and Mechanisms</i> , 2nd Edition, McGraw-Hill, Inc., 1995, p.115.
vm240	Thermal Expansion of Rigid Beams in a Composite Bar <u>SOLID185</u> <u>MPC184</u>	A composite bar consists of two base materials with 25 rigid beams embedded along its length. A coefficient of thermal expansion is defined for only the rigid beams. Compare the stresses resulting in both solid composite materials when a temperature is applied.	J.M. Gere, S.P. Timoshenko, <i>Mechanics of Materials</i> , 2nd Edition, PWS Publishers, 1984, p. 20-21,71

vm241	Static Force Computation of a 3-D Solenoid Actuator <u>SOLID231</u> <u>(SOLID232</u> <u>SOLID236</u> <u>SOLID237</u> <u>MESH200</u>	For the given solenoid actuator with an applied total coil current of 5000 A-turns, find the magnetic flux density (Bz) of the Pole, the magnetic flux density (Bz) of the Arm, and the Magnetic Force in the Z-direction. The center pole and yoke are made of steel characterized by the B-H curve	N.Takahashi, T. Nakata, and H. Morishige, "Summary of Results for Problem 20 (3-D Static Force Problem)", COMPEL, Vol.14 (1995), pp. 57-75.
vm244	Modal Analysis of a Cyclic Symmetric Annular Plate <u>SOLID185</u> <u>SOLID186</u> <u>SOLID187</u> <u>SHELL181</u> <u>SOLSH190</u> <u>SHELL281</u>	The fundamental natural frequency of an annular plate is determined using a mode-frequency analysis. The lower bound is calculated from the natural frequency of the annular plates, which are free on the inner radius and fixed on the outer. The bounds for the plate frequency are compared to the theoretical results.	R. D. Blevins, <i>Formulas for Natural Frequency and Mode Shape</i> , New York, NY, VanNostrand Reinhold Publishing Inc., 1979, pp. 246-247, 286-287.
vm247	Campbell Diagrams and Critical Speeds Using Symmetric Bearings <u>BEAM188</u> <u>MASS21</u> <u>COMBIN14</u>	A rotor-bearing system is analyzed to determine the whirl speeds. The distributed rotor was modeled as a configuration of six elements with each element composed of subelements. Two undamped linear bearings were located at positions four and six. Modal analysis is performed on rotor bearing system with multiple load steps to determine the critical speeds and Campbell values for the system.	Nelson and McVaugh, "The Dynamics of Rotor-Bearing Systems Using Finite Elements", Journal of Engineering for Industry, May 1976.
vm248	Delamination Analysis of Double Cantilever Beam <u>PLANE182</u> <u>INTER202</u> <u>CONTA171</u> <u>PLANE183</u> <u>INTER203</u> <u>CONTA172</u> <u>SOLID185</u> <u>INTER205</u> <u>CONTA173</u> <u>TARGE169</u> <u>TARGE170</u>	A double cantilever beam of length l , width w and height h with an initial crack of length a at the free end is subjected to a maximum vertical displacement U_{max} at top and bottom free end nodes. Determine the vertical reaction at point P based on the vertical displacement for the interface model.	G. Alfano and M. A. Crisfield <i>Finite Element Interface Models for the Delamination Analysis of Laminated Composites: Mechanical and Computational Issues</i> , International Journal for Numerical Methods in Engineering, Vol. 50, pp. 1701-1736 (2001).

vm250	Gasket Material Under Uniaxial Compression Loading - 3-D Analysis <u>SOLID185</u> <u>SOLID186</u> <u>INTER195</u> <u>INTER194</u>	A thin interface layer of thickness t is defined between two blocks of length L , width W , and height H placed on top of each other. The blocks are constrained on the left, bottom, and back faces and loaded with pressure P on the top face. Determine the pressure-closure response for gasket elements.	Any Nonlinear Material Verification Text
vm251	Shape Memory Alloy Under Uniaxial Tension Load <u>PLANE182</u> <u>PLANE183</u> <u>SOLID185</u>	A square block of length, height and width L is constrained in the X-direction on the left face, constrained in the Y-direction rear on the bottom face and constrained in the Z-direction on the rear face (3-D case only). It is uniaxially loaded with tensile stress of s and unloaded on the top face. Determine the stress-strain response for a Ni-Ti alloy.	Ferdinando Auricchio, Robert L. Taylor, and Jacob Lubliner, <i>Shape-memory alloys: macromodelling and numerical simulations of the superelastic behavior</i> , Comput. Methods Appl. Mech. Engrg., Vol. 146, pp. 281-312 (1997).
vm253	Gurson Hydrostatic Tension Benchmark - 3-D Analysis <u>SOLID185</u> <u>SOLID186</u>	The model is a three dimensional bin with all sides equal to unity. An applied displacement of 0.15" is applied at the nodes corresponding to $x = 1$, $y = 1$, and $z = 1$. To prevent rigid body motion, the model is constrained in the x direction at $x = 0$, y -direction at $y = 0$, and z -direction at $z = 0$.	N. Aravas, "On the Numerical Integration of a Class of Pressure Dependent Plasticity Models", <i>International Journal for Numerical Methods in Engineering</i> , Vol. 24, pp. 1395-1416, Section 5.2, Figure 7 (1987).
vm254	Campbell Diagrams and Critical Speeds Using Symmetric Orthotropic Bearings <u>PIPE16</u> <u>PIPE288</u> <u>MASS21</u> <u>COMBI214</u>	A rotor-bearing system is analyzed to determine the forward and backward whirl speeds. The distributed rotor was modeled as a configuration of six elements with each element composed of subelements. Two symmetric orthotropic bearings were located at positions four and six. Modal analysis is performed on rotor bearing system with multiple load steps to determine the whirl speeds and Campbell values for the system.	Nelson, H.D., McVaugh, J.M., "The Dynamics of Rotor-Bearing Systems Using Finite Elements", <i>Journal of Engineering for Industry</i> , Vol 98, pp. 593-600, 1976

vm256	Fracture Mechanics Stress for a Crack in a Plate using <u>CINT</u> Command <u>PLANE183</u> <u>SOLID185</u> <u>SOLID186</u>	A long plate with a center crack is subjected to an end tensile stress σ . Symmetry boundary conditions are considered and the fracture mechanics stress intensity factor K_I is determined using <u>CINT</u> command.	W.F.Brown, Jr., J.E.Srawley, <i>Plane strain crack toughness testing of high strength metallic materials</i> , ASTM STP-410, (1966).
vm257	Transient Analysis of a Swing with Two Rigid Links and Beam <u>BEAM188</u> <u>MPC184</u> <u>TARGE170</u>	The swing consists of a long aluminum beam of rectangular cross-section (width = 1mm, depth = 5 mm) and a mid-span mass (mass = 0.5 kg). The mass is rigidly connected to the beam at its mid-span position. The beam is suspended at each end by two rigid links, and is initially at rest. The rigid links impose a kinematic constraint corresponding to fixed distance between points O_1 and A, and O_2 and E of 0.36 and 0.72, respectively. The points B and D indicate the quarter and three quarter span points of the beam, respectively. The loading of the system consists of a triangular pulse in the direction applied at the mid-span mass. This pulse starts at time $t = 0$ s, reaches a peak value of 2N at $t = 0.128$ s and goes back to zero at $t = 0.256$ s.	O.A. Bauchau, G. Damilano, and N.J. Theron <i>Numerical Integration of Non-Linear Elastic Multi-Body Systems</i> , International Journal for Numerical Methods in Engineering, Vol. 38, 2727-2751 (1995).

vm259	Missing Mass with Rigid Responses Effects in Spectrum Analysis for BM3 Piping Model <u>PIPE16</u> <u>PIPE18</u> <u>COMBIN14</u>	<p>The BM3 piping model is meshed with <u>PIPE16</u> and <u>PIPE18</u> elements. The model is supported by elastic spring-damper elements (<u>COMBIN14</u>). Lumped mass matrix formulation is used in the modal analysis. Single point response spectrum analysis is then performed with an acceleration input spectra defined by 75 points (<u>FREQ</u> and <u>SV</u>). The first 14 modes are included in the spectrum analysis. The model is excited in X direction and the modal responses are combined using <u>SRSS</u> mode combination method with displacement solution output. The analysis is performed for three cases:</p> <p>With missing mass effect (ZPA=0.54g).</p> <p>With missing mass (ZPA=0.54g) and rigid responses effect (Lindley Method).</p> <p>With missing mass (ZPA=0.54g) and rigid responses effect (Gupta Method, F1=2.8Hz and F2=6.0Hz).</p>	R. Morante, Y. Wang, <i>Reevaluation of regulatory guidance on modal response combination methods for seismic response spectrum analysis</i> (NUREG/CR-6645), Brookhaven National Laboratory, Dec 1999.
vm261	Rotating Beam with Internal Viscous Damping <u>BEAM188</u> <u>COMBI214</u>	A beam with internal viscous damping is simply supported by means of two isotropic undamped bearings. Modal analysis is performed with multiple load steps to determine the critical speeds and logarithmic decrement of the system.	E.S. Zorzi, H.D. Nelson, "Finite element simulation of rotor-bearing systems with internal damping", <i>ASME Journal of Engineering for Power</i> , Vol. 99, 1976, pg. 71-76.

vm265	Elastic Rod Impacting a Rigid Wall <u>SHELL181</u> <u>CONTA177</u> <u>TARGE170</u>	A linear elastic prismatic rod is moving with an initial velocity and is impacting a rigid wall. The shock wave created from impact travels as a compression wave through the rod. During this time, the rod remains in contact with the rigid wall. The compression wave is then reflected as a dilatational wave upon reaching the free end of the rod and travels back to the contact surface. The rod gets separated from the rigid wall once the dilatational wave reaches the contact surface. The time at impact and at separation is determined from the analysis along with corresponding displacements, velocities and normal contact forces at the contact surface and compared to the solutions given in the reference. The time history plots are also compared to the reference plots.	N.J.Carpenter, R.L. Taylor and M.G. Katona, "Lagrange Constraints For Transient Finite Element Surface Contact", International Journal for Numerical Methods in Engineering, vol.32, 1991. Pg. 103-128.
vm266	3-D Crossing Beams in Contact with Friction <u>BEAM188</u> <u>CONTA176</u> <u>TARGE170</u>	Two orthogonal beams with similar cross section and with an initial out-of-plane displacement are brought into contact by undergoing large displacements in 3-D space. Normal and frictional contact forces are calculated at 0.5, 0.66, 0.83, and 1 second, and then compared against reference values.	G. Zavarise and P. Wriggers, "Contact with friction between beams in 3-D space", International Journal for Numerical Methods in Engineering, 2000, vol.49, pp. 977-1006.
vm272	2-D and 3-D Frictional Hertz Contact <u>PLANE182</u> <u>CONTA171</u> <u>TARGE169</u> <u>SURF153</u> <u>SOLID185</u> <u>CONTA173</u> <u>TARGE170</u> <u>SURF154</u>	Two parallel linear elastic half cylinders of radius R are pressed by a small distributed pressure p. A tangential pressure, q, is then applied to cause friction at the contact interface. The bottom of the lower cylinder is fixed in all directions. Determine the contact pressure and friction results across the contact interface.	Two Dimensional Mortar Contact Methods for Large Deformation Frictional Sliding, International Journal for Numerical Methods in Engineering Vol.62, pp 1183-1225.

vm273	Shape Memory Alloy With Thermal Effect Under Uniaxial Loading <u>SOLID185</u>	A block is made of shape memory alloy material. One cycle of uniaxial displacement loading is applied in vertical direction. The whole process includes tension, unload, compression, and unload. The whole loading history repeats with body temperature 285.15K and 253.15K, respectively. The stress history is obtained and compared against the reference solution.	Auricchio, F. et al. <i>"Improvements and algorithmical considerations on a recent three-dimensional model describing stress-induced solid phase transformation"</i> . <i>International Journal for Numerical Methods in Engineering</i> , 55. 1225-1284. 2002
vm274	Stabilizing Squeal Damping <u>SOLID185</u> <u>CONTA173</u> <u>TARGE170</u> <u>COMBIN14</u> <u>MASS21</u>	A rigid block (Young's modulus E, Poisson ratio ν , density ρ , length of edge a, area A) is elastically supported by a spring-damper element and guided by a rail with a velocity u . The whole assembly is sliding on the rough ex-ey-plane (coefficient of friction μ , normal pressure p). Linear perturbation modal analysis is performed using the DAMP eigensolver to determine the damped frequency and modal damping ratio, which is then compared against analytical results.	Any Dynamics Textbook
vm277	Hall Plate in a Uniform Magnetic Field <u>SOLID236</u> <u>CIRCU124</u> <u>MESH200</u>	A series of static electromagnetic analyses is performed on a plate with length 2a, height 2b, and thickness c to determine the Hall voltage produced by a uniform magnetic field B perpendicular to the plate surfaces	Meijer, G. <i>Smart Sensor Systems</i> . John Wiley & Sons, Ltd. 2008, p. 252.
vm279	T-Stress for a Crack in a Plate Using the CINT Command <u>PLANE183</u> <u>SOLID185</u> <u>SOLID186</u>	A rectangular plate with a center crack is subjected to an end tensile stress σ Symmetry boundary conditions are considered and T-Stress is determined using the CINT command.	Fett, T., <i>Stress Intensity Factors, T-Stresses, Weight Functions</i> , Institute of Ceramics in Mechanical Engineering, University of Karlsruhe, 2008, pp. 151-152

vm281	Effect of Stress Stiffening and Spin Softening on a Rotating Plate <u>SHELL181</u> <u>SOLID185</u>	A steel plate, clamped on one edge and free on the other edges, is rotating about an offset axis. The first bending frequency is determined as a function of the rotational velocity. The analysis is done for two cases: rotation about the Z-axis and about the X-axis.	Lawrence, C., Aiello, R. A., Ernst, M. A., McGee, O. G., "A NASTRAN Primer for the Analysis of Rotating Flexible Blades", <i>NASA Technical Memorandum 89861</i> , 1987, p. 14
vm282	Mode-Superposition Response Analysis of a Piston-Fluid System <u>FLUID30</u> <u>MASS21</u> <u>COMBIN14</u> <u>CONTA174</u> <u>TARGE170</u>	A simple piston-fluid system is modeled using a spring damper element (<u>COMBIN14</u>) for the piston, fluid elements (<u>FLUID30</u>) for the fluid column, and a mass element (<u>MASS21</u>) for the mass of the piston,. The contact between the piston and the fluid column is established using the surface-to-surface contact element (<u>CONTA174</u>).	Axisa, F., Antunes, J., <i>Modelling Mechanical Systems: Fluid-Structure Interaction</i> , 2006, p. 486
vm284	Acceleration Solution in Response Spectrum Analysis Using Missing Mass Method <u>BEAM188</u> <u>MASS21</u>	Single point acceleration response spectrum analysis is performed on a vertical tank model that is 200 inches tall and 35 inches in diameter by exciting the structure in the global Z-direction. The tank is supported by a braced leg support and is filled with a fluid with a specific gravity of 1.57. The spectrum analysis is performed with the first four modes and missing mass to account for the higher modes. The modes are combined using the <u>SRSS</u> mode combination method and the absolute acceleration at different elevation points of the structure is obtained by summing the <u>SRSS</u> modal response with the absolute missing mass response. The accelerations are compared against the reference values shown in Column 9 of Table 1 in the reference document.	Biswas, J.K, Duff, C.G., "Response Spectrum Method with Residual Terms", <i>ASME Publications</i> , April 1978.

vm286	Wear of a Block Under Uniform Compression <u>PLANE182</u> <u>CONTA171</u> <u>TARGE169</u> <u>SOLID185</u> <u>CONTA173</u> <u>TARGE170</u>	Wear analysis is performed on a block with length L in contact with a rigid plate using a frictionless standard contact pair. In the first load step, a displacement load is applied on one face of the block to compress the block onto the rigid plate. In the second load step, displacement is applied on the rigid plate to make it slide, resulting in wear of the block. The contact pressure and amount of wear on the block is computed and compared against the analytical solution.	Any standard engineering textbook.
vm292	Interference Fit Between Two Cylinders <u>SOLID185</u> <u>CONTA173</u> <u>TARGE170</u>	Two cylinders connected by means of standard frictionless contact are modeled with an interference fit between them. Static analysis is performed to predict the contact pressure between the two cylinders.	Budynas, R.G., Nisbett, J.K., <i>Shigley's Mechanical Engineering Design</i> , 9th edition, pg. 116, 2011.

Table 2: SAP2000 Summary of Group 1 (FRAME) Verification Problems

Problem No.	Problem Title	SAP2000 Frame Element Features Tested	Method of Independent Verification
1-001	General Loading	<ul style="list-style-type: none"> · Calculation and application of self load · Projected, uniformly distributed load · Application of uniformly distributed load in global coordinates · Uniformly distributed load in frame object local coordinates · Trapezoidal and triangular distributed load on frames · Joint moments and forces · Static analysis of frames under all of these loading types 	Hand calculation using the unit load method described on page 244 in Cook and Young 1985.
1-002	Temperature Loading	<ul style="list-style-type: none"> · The specification of joint patterns · The application of temperature increase · Transverse temperature gradient · The calculation of displacements in free expansion · Reaction forces in restrained case caused by temperature loads 	Hand calculation using standard thermal expansion formulas and using Table 3 items 6a and 6c on page 107 in Roark and Young 1975.
1-003	Distributed and Concentrated Moments	The application of: <ul style="list-style-type: none"> · Distributed moments (uniform, trapezoidal, triangular) to frame objects · Concentrated moments to frame objects 	Hand calculation using equation 8.1.3 on page 284 in Cook and Young 1985.
1-004	Rotated Local Axes	Frame local axes rotated from global axes. Use of AISC sections.	Hand calculation using the beam deflection formulas in Table 3 item 1a and Table 3 item 2a on pages 96 and 98, respectively, in Table 3 in Roark and Young 1975.

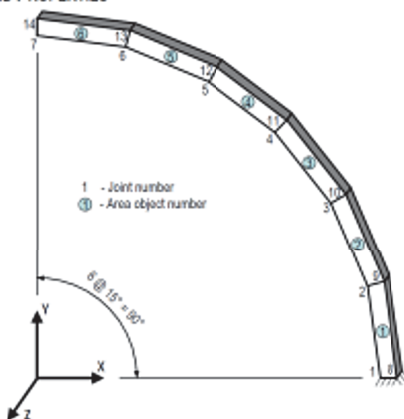
1-005	Displacement Loading	<ul style="list-style-type: none"> · Settlement of support in frame structures · Rotation of support in frame structures · Settlement of support with linear (translational) spring · Rotation of support with rotational spring · Skewed supports · Skewed support settlement 	Hand calculation using the unit load method described on page 244 in Cook and Young 1985.
1-006	Non-Prismatic Sections and Automatic Frame Subdivision	<ul style="list-style-type: none"> · Structural behavior of a non-prismatic frame section · Self-weight calculations · Linear variation of section area · Linear, parabolic and cubic variation of moment of inertia · Linear variation of section torsional constant · Automatic frame subdivision 	Hand calculation using the unit load method described on page 244 in Cook and Young 1985.
1-007	End Releases	<p>The end releases in a frame element, including</p> <ul style="list-style-type: none"> Axial release Shear release Bending release <p>The related frame static analysis</p>	Hand calculation using basic statics.
1-008	Partial Fixity End Releases	<p>The partial fixity end releases in a frame element, including</p> <ul style="list-style-type: none"> Shear partial fixity Bending partial fixity <p>The application of gravity load to a frame object</p>	Hand calculation using the unit load method described on page 244 in Cook and Young 1985.
1-009	Prestress Applied To Frame Objects	<ul style="list-style-type: none"> · Prestress tendon with parabolic tendon profile and different eccentricities at the two ends · Prestress tendon modeled using loads · Prestress tendon modeled as elements · Prestress losses 	Hand calculation using basic principles and the unit load method described on page 244 in Cook and Young 1985.

1-010	End Offsets	The use of end offsets in frames, including Non-rigid offsets Partially rigid offsets Fully rigid offsets The effect of end offsets on the frame static analysis results	Hand calculation using the unit load method described on page 244 in Cook and Young 1985.
1-011	Insertion Point	Cardinal point Joint offsets	Hand calculation using statics.
1-012	No Tension and No Compression Frame Objects	Tension and compression limits for frame objects End releases	Hand calculation using the unit load method described on page 244 in Cook and Young 1985 together with statics.
1-013	Simply Supported Beam on Elastic Foundation	Frame line spring assignments Static analysis of beam on elastic foundation Automatic frame subdivision	Hand calculated using formulas presented in Problem 3 on page 23 of Timoshenko 1956.
1-014	Eigenvalue Problem	Eigenvalue analysis of a frame with unequal moment of inertia values ($I_{22} \neq I_{33}$) for bending modes Automatic frame subdivision	Hand calculation based on formulas presented on page 313 of Clough and Penzien 1975.
1-015	Steady State Harmonic Loads	Steady state analysis of frame systems Time history analysis of frame systems with periodic loading Line mass assignment to frame objects Automatic frame subdivision	Comparison with illustrative example 20.2 on page 434 of Paz 1985.
1-016	Tension Stiffening Using P-Delta Analysis	P-Delta force assignment to frame objects Nonlinear static analysis using the P-Delta option Automatic frame subdivision	Hand calculation using equation 23 on page 28 and equations 43 and 45 on page 43 of Timoshenko 1956.
1-017	Vibration of a String Under Tension	Static nonlinear analysis using the P-Delta option to provide tension stiffening Modal analysis of frame for eigenvalues	Hand calculation using vibration theory presented on pages 506 through 510 of Kreyszig 1983.

1-018	Bending, Shear and Axial Deformations in a Rigid Frame	Calculation of bending, shear and axial deformations in a rigid frame Frame property modification factors	Hand calculation using the unit load method described on page 244 in Cook and Young 1985.
1-019	Buckling of a Rigid Frame	Buckling analysis of a rigid frame Automatic frame subdivision	Hand calculation using formulas presented in Article 2.4 on pages 62 through 66 of Timoshenko and Gere 1961.
1-020	Response Spectrum Analysis of a Two-Dimensional Rigid Frame	Modal analysis of frame for eigenvalues and time periods Response spectrum analysis Joint masses	Comparison with example 13.11 on page 521 of Chopra 1995.
1-021	Bathe and Wilson Eigenvalue Problem	Modal analysis for eigenvalues Line mass assignment to frame objects	Comparison with results published in Bathe and Wilson 1972 and comparison with results from another computer program published in Peterson 1981.
1-022	Two-Dimensional Moment Frame with Static and Dynamic Loads	<ul style="list-style-type: none"> · Diaphragm constraint · Joint force assignments · Joint mass assignments · Modal analysis for eigenvalues · Response spectrum analysis · Modal time history analysis for base excitation · Direct integration time history analysis for base excitation 	Comparison with results from another computer program published by Engineering/Analysis and Computers/ Structures International.
1-023	ASME Eigenvalue Problem	Three-dimensional frame analysis Modal analysis using eigenvectors Joint mass assignments	Comparison with results from another computer program published in Peterson 1981 and in DeSalvo and Swanson 1977.
1-024	Response Spectrum Analysis of a Three-Dimensional Moment Frame	<ul style="list-style-type: none"> · Three-dimensional frame analysis · Modal analysis using eigenvectors · Rigid diaphragm constraint · Joint mass assignments · Response spectrum analysis 	Comparison with results from another computer program published in Peterson 1981.

1-025	Response Spectrum Analysis of a Three-Dimensional Braced Frame	<ul style="list-style-type: none"> · Three-dimensional frame analysis · Modal analysis using eigenvectors · Rigid diaphragm constraint · Joint mass assignments · Response spectrum analysis 	Comparison with results from another computer program published in Peterson 1981.
1-026	Moment and Shear Hinges	Static nonlinear analysis of a frame structure using moment and shear hinges	Hand calculation using the unit load method described on page 244 in Cook and Young 1985 together with basic deflection formulas and superposition.
1-027	Construction Sequence Loading	Nonlinear static analysis using the construction sequence loading option Frame end releases	Hand calculation using the unit load method described on page 244 in Cook and Young 1985 together with basic deflection formulas.
1-028	Large Axial Displacements	Static nonlinear analysis of frame structure with large axial displacements using the SAP2000 P-Delta plus large displacements option Frame end releases	Hand calculation using basic statics.
1-029	Large Bending Displacements	Static nonlinear analysis of frame structure with large bending displacements using the SAP2000 P-Delta plus large displacements option	Hand calculation and Equation 4 in Article 7.1 of Chapter 7 on page 91 of Roark and Young 1975.
1-030	Moving Loads	Moving load case Multi-step static load case for vehicles	Comparison with results published in Appendix A of AASHTO 1990 and hand calculation.

Table 3: SAP2000 Summary of Group 2 (SHELL) Verification Problems

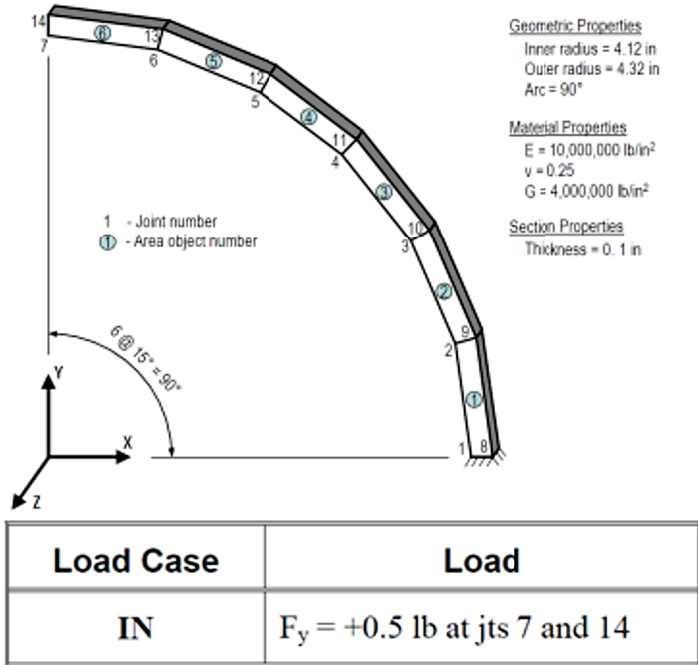
Problem No.	Problem Title	SAP2000 Shell Element Features Tested	Method of Independent Verification						
2-001	Patch Test With Prescribed Displacements	<ul style="list-style-type: none">Membrane analysis using shell elementsPlate bending analysis using shell elementsThin-plate optionThick-plate optionJoint displacement loading	Hand calculation based theory in Timoshenko and Goodier 1951 and Timoshenko and Woinowsky-Krieger 1959. Results also published in MacNeal and Harder 1985.						
2-002	Straight Beam with Static Loads	<ul style="list-style-type: none">Membrane analysis using shell elementsPlate bending analysis using shell elementsEffect of shell element aspect ratioEffect of geometrical distortion of shell element from rectangularJoint force loading	Hand calculation using the unit load method described on page 244 in Cook and Young 1985 and using formulas from Roark and Young 1975. Results also published in MacNeal and Harder 1985.						
2-003	Curved Beam with Static Loads	<div><ul style="list-style-type: none">Membrane analysis using shell elementsPlate bending analysis using shell elementsJoint force loading<div><p>GEOMETRY AND PROPERTIES</p><p>1 - Joint number ⑬ - Area object number</p><p>Geometric Properties Inner radius = 4.12 in Outer radius = 4.32 in Arc = 90°</p><p>Material Properties E = 10,000,000 lb/in² ν = 0.25 G = 4,000,000 lb/in²</p><p>Section Properties Thickness = 0.1 in</p></div><table><thead><tr><th>Load Case</th><th>Load</th></tr></thead><tbody><tr><td>IN</td><td>F_y = +0.5 lb at jts 7 and 14</td></tr><tr><td>OUT</td><td>F_z = +0.5 lb at jts 7 and 14</td></tr></tbody></table></div>	Load Case	Load	IN	F _y = +0.5 lb at jts 7 and 14	OUT	F _z = +0.5 lb at jts 7 and 14	Hand calculation using the unit load method described on page 244 in Cook and Young 1985. Results also published in MacNeal and Harder 1985.
Load Case	Load								
IN	F _y = +0.5 lb at jts 7 and 14								
OUT	F _z = +0.5 lb at jts 7 and 14								

2-004	Twisted Beam with Static Loads	<ul style="list-style-type: none"> · Membrane analysis using shell elements · Plate bending analysis using shell elements · Joint force loading 	Hand calculation using the unit load method described on page 244 in Cook and Young 1985. Results also published in MacNeal and Harder 1985.
2-005	Rectangular Plate with Static Loads	<ul style="list-style-type: none"> · Plate bending analysis using shell elements · Uniform load applied to shell elements · Joint force loading 	Hand calculation based theory in Timoshenko and Woinowsky-Krieger 1959. Results also published in MacNeal and Harder 1985.
2-006	Scordelis-Lo Roof with Static Loads	<ul style="list-style-type: none"> · Three-dimensional analysis using shell elements · Self-weight applied to shell elements · Gravity load applied to shell elements · Uniform load applied to shell elements 	Some results published in MacNeal and Harder 1985. Other results scaled from plotted results in Zienkiewicz 1977 that were calculated using theory presented in Scordelis and Lo 1964.
2-007	Hemispherical Shell Structure with Static Loads	<ul style="list-style-type: none"> · Three-dimensional analysis using shell elements · Joint local axes · Joint force loads 	Result published in MacNeal and Harder 1985.
2-008	Cantilever Plate Eigenvalue Problem	<ul style="list-style-type: none"> · Eigenvalue analysis using shell elements · Area object mass assignment · Area object automatic mesh · Area object stiffness modifiers 	Hand calculation using Table 7.7 on page 7-30 of Harris and Crede 1976.
2-009	Plate on Elastic Foundation	<ul style="list-style-type: none"> · Plate bending analysis using shell elements · Area object spring assignment · Joint force loads 	Hand calculation using equation 185 on page 275 of Timoshenko and Woinowsky-Krieger 1959.
2-010	Cylinder with Internal Pressure	<ul style="list-style-type: none"> · Three-dimensional analysis using shell elements · Surface pressure load applied to shell elements · Joint local axes 	Hand calculation using item 1b in Table 29 on page 448 of Roark and Young 1975.

2-011	ASME Cooling Tower Problem with Static Wind Pressure	<ul style="list-style-type: none"> Three-dimensional analysis using shell elements Joint patterns Shell element surface pressure load using joint pattern 	Results scaled from plotted results in Zienkiewicz 1977 that were calculated using theory presented in Albasiny and Martin 1967.
2-012	Plate Bending when Shear Deformations Are Significant	<ul style="list-style-type: none"> Plate bending analysis of shell elements when shear deformations are significant Area object stiffness modifiers Frame distributed loads 	Results published in example shown on page 376 of Roark and Young 1975.
2-013	Temperature Load that Is Constant Through Shell Thickness	<ul style="list-style-type: none"> Temperature loading for shell elements 	Hand calculation using equation 1.3.4 on page 9 of Cook and Young 1985.
2-014	Temperature Gradient Through Shell Thickness	<ul style="list-style-type: none"> Temperature gradient loading for shell elements Area object local axes Joint local axes 	Hand calculation using formulas presented in item 8e of Table 24 on page 361 of Roark and Young 1975.
2-015	Orthotropic Plate	<ul style="list-style-type: none"> Plate bending analysis of shells Orthotropic material properties Area object stiffness modifiers 	Hand calculated using theory presented in Chapter 6 of Ugural 1981.
2-016	Out-of-Plane Buckling	<ul style="list-style-type: none"> Buckling analysis of shells Automatic area meshing (N x N) with added restraints Joint springs Frame property modifiers Frame distributed load Frame automatic subdivide at intermediate joints 	Hand calculated using theory presented in Timoshenko and Gere 1961.
2-017	In-Plane Buckling	<ul style="list-style-type: none"> Buckling analysis of shells Joint force loads Active degrees of freedom 	Hand calculated using equation 2-4 on page 48 of Timoshenko and Gere 1961.
2-018	Large Axial Displacements	<ul style="list-style-type: none"> Static nonlinear analysis of shell structure with large axial displacements using the SAP2000 P-Delta plus large displacements option Joint constraints 	Hand calculation using basic statics.
2-019	Large Bending Displacements	<ul style="list-style-type: none"> Static nonlinear analysis of shell structure with large bending displacements using the SAP2000 P-Delta plus large displacements option Automatic area meshing 	Hand calculation and Equation 4 in Article 7.1 of Chapter 7 on page 91 of Roark and Young 1975.

2-020	Prestress Applied to Area Objects	<ul style="list-style-type: none"> · Prestress tendon with parabolic tendon profile and different eccentricities at the two ends · Prestress tendon modeled using loads and applied to area objects · Prestress tendon modeled as elements and applied to area objects · Prestress losses 	Hand calculation using basic principles and the unit load method described on page 244 in Cook and Young 1985.
-------	---	---	--

Table 4: SAP2000 Summary of Group 3 (PLANE) Verification Problems

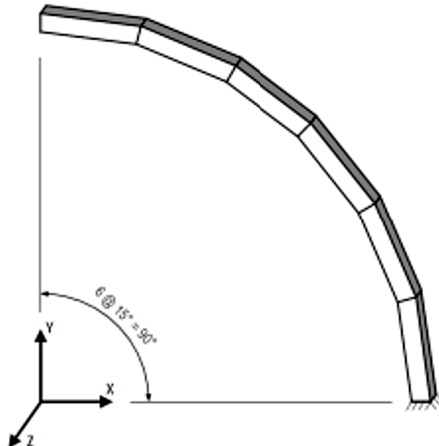
Problem No.	Problem Title	SAP2000 Plane Element Features Tested	Method of Independent Verification				
3-001	Patch Test With Prescribed Displacements	<ul style="list-style-type: none">Membrane analysis using plane stress elementsIncompatible bending mode option for plane elementsJoint displacement loading	Hand calculation based theory in Timoshenko and Goodier 1951. Results also published in MacNeal and Harder 1985.				
3-002	Straight Beam with Static Loads	<ul style="list-style-type: none">Membrane analysis using plane elementsEffect of plane element aspect ratioEffect of geometrical distortion of plane element from rectangularJoint force loading	Hand calculation using the unit load method described on page 244 in Cook and Young 1985 and using formulas from Roark and Young 1975. Results also published in MacNeal and Harder 1985.				
3-003	Curved Beam with Static Loads	<ul style="list-style-type: none">Membrane analysis using plane stress elementsJoint force loading <p>GEOMETRY AND PROPERTIES</p>  <p>1 - Joint number ① - Area object number</p> <p>Geometric Properties Inner radius = 4.12 in Outer radius = 4.32 in Arc = 90°</p> <p>Material Properties E = 10,000,000 lb/in² ν = 0.25 G = 4,000,000 lb/in²</p> <p>Section Properties Thickness = 0.1 in</p> <table><thead><tr><th>Load Case</th><th>Load</th></tr></thead><tbody><tr><td>IN</td><td>F_y = +0.5 lb at jts 7 and 14</td></tr></tbody></table>	Load Case	Load	IN	F _y = +0.5 lb at jts 7 and 14	Hand calculation using the unit load method described on Page 244 in Cook and Young 1985. Results also published in MacNeal and Harder 1985.
Load Case	Load						
IN	F _y = +0.5 lb at jts 7 and 14						

3-004	Thick-Walled Cylinder	<ul style="list-style-type: none"> · Analysis using plane stress elements · Analysis using plane strain elements · Plane surface pressure load 	Hand calculation based on theory in Timoshenko 1956 and based on formulas in Roark and Young 1975. Results also published in MacNeal and Harder 1985.
3-005	Pore Pressure	<ul style="list-style-type: none"> · Pore pressure loading for planes · Joint pattern 	Hand calculation using basic principles.

Table 5: SAP2000 Summary of Group 4 (ASOLID) Verification Problems

Problem No.	Problem Title	SAP2000 ASOLID Element Features Tested	Method of Independent Verification
4-001	Soil Supporting Uniformly Loaded Circular Footing	<ul style="list-style-type: none"> Analysis using asolid elements Asolid surface pressure load Incompatible bending modes for asolid objects 	Hand calculation based on data presented in Poulos and Davis 1974.
4-002	Thick-Walled Cylinder	<ul style="list-style-type: none"> Analysis using asolid elements Asolid surface pressure load 	Hand calculation based on theory in Timoshenko 1956. Results also published in MacNeal and Harder 1985.
4-003	Rotating Annular Disk	<ul style="list-style-type: none"> Analysis using asolid elements Asolid rotation load 	Hand calculation based on equations presented in Item 8 on page 567 of Roark and Young 1975.
4-004	Pore Pressure	<ul style="list-style-type: none"> Pore pressure loading for asolids Joint pattern 	Hand calculation using basic principles.

Table 6: SAP2000 Summary of Group 5 (SOLID) Verification Problems

Problem No.	Problem Title	SAP2000 Solid Element Features Tested	Method of Independent Verification						
5-001	Patch Test With Prescribed Displacements	<ul style="list-style-type: none">· Patch test using solid elements· Joint displacement loading	Results also published in MacNeal and Harder 1985.						
5-002	Straight Beam with Static Loads	<ul style="list-style-type: none">· Solid object bending with and without the incompatible modes option· Effect of solid object aspect ratio· Effect of geometrical distortion of solid object from a cube· Joint force loading	Hand calculation using the unit load method described on page 244 in Cook and Young 1985. Results also published in MacNeal and Harder 1985.						
5-003	Curved Beam with Static Loads	<div><ul style="list-style-type: none">· Solid object bending with the incompatible bending modes option· Joint force loading<p>GEOMETRY AND PROPERTIES</p><p><u>Geometric Properties</u> Inner radius = 4.12 in Outer radius = 4.32 in Arc = 90°</p><p><u>Material Properties</u> E = 10,000,000 lb/in² ν = 0.25 G = 4,000,000 lb/in²</p><p><u>Section Properties</u> Thickness = 0.1 in</p><table><thead><tr><th>Load Case</th><th>Load</th></tr></thead><tbody><tr><td>IN</td><td>F_y = +0.25 lb at each of four corner joints at tip</td></tr><tr><td>OUT</td><td>F_z = +0.25 lb at each of four corner joints at tip</td></tr></tbody></table></div>	Load Case	Load	IN	F _y = +0.25 lb at each of four corner joints at tip	OUT	F _z = +0.25 lb at each of four corner joints at tip	Hand calculation using the unit load method described on page 244 in Cook and Young 1985. Results also published in MacNeal and Harder 1985.
Load Case	Load								
IN	F _y = +0.25 lb at each of four corner joints at tip								
OUT	F _z = +0.25 lb at each of four corner joints at tip								
5-004	Twisted Beam with Static Loads	<ul style="list-style-type: none">· Solid object bending and twist with the incompatible bending modes option· Joint force loading	Hand calculation using the unit load method described on page 244 in Cook and Young 1985. Results also published in MacNeal and Harder 1985.						

5-005	Rectangular Plate with Static Loads	<ul style="list-style-type: none"> · Plate bending analysis using solid elements · Surface pressure load applied to solid objects · Joint force loading 	Hand calculation based theory in Timoshenko and Woinowsky-Krieger 1959. Results also published in MacNeal and Harder 1985.
5-006	Scordelis-Lo Roof with Static Loads	<ul style="list-style-type: none"> · Three-dimensional analysis using solid objects · Self-weight applied to solid objects · Gravity load applied to shell objects 	Some results published in MacNeal and Harder 1985. Other results scaled from plotted results in Zienkiewicz 1977 that were calculated using theory presented in Scordelis and Lo 1964.
5-007	Hemispherical Dome Structure with Static Loads	<ul style="list-style-type: none"> · Three-dimensional analysis using solid elements · Joint force loads 	Results published in MacNeal and Harder 1985.
5-008	Thick-Walled Cylinder	<ul style="list-style-type: none"> · Analysis using solid elements · Solid surface pressure load · Joint local axes 	Hand calculation based on theory in Timoshenko 1956. Results also published in MacNeal and Harder 1985.
5-009	Prestress Applied to Solid Objects	<ul style="list-style-type: none"> · Prestress tendon with parabolic tendon profile and different eccentricities at the two ends · Prestress tendon modeled using loads and applied to solid objects · Prestress tendon modeled as elements and applied to solid objects · Prestress losses 	Hand calculation using basic principles and the unit load method described on page 244 in Cook and Young 1985.
5-010	Buckling	<ul style="list-style-type: none"> · Buckling analysis of solids · Joint force loads · Active degrees of freedom 	Hand calculation using equation 2-4 on page 48 of Timoshenko and Gere 1961.
5-011	Temperature Load	<ul style="list-style-type: none"> · Temperature loading for solid elements 	Hand calculation using equation 1.3.4 on page 9 of Cook and Young 1985.

5-012	Plate on Elastic Foundation	<ul style="list-style-type: none"> · Plate bending analysis using solid elements · Solid object surface spring assignment · Solid object automatic mesh · Joint force loads 	Hand calculation using equation 185 on page 275 of Timoshenko and Woinowsky-Krieger 1959.
5-013	Pore Pressure	<ul style="list-style-type: none"> · Pore pressure loading for solids · Solid local axis assignments · Joint pattern 	Hand calculation using basic principles.

Table 7: SAP2000 Summary of Group 6 (LINK) Verification Problems

Problem No.	Problem Title	SAP2000 Link Element Features Tested	Method of Independent Verification
6-001	Linear Link with Ramp Loading	<ul style="list-style-type: none"> · Linear links · Modal load case for eigenvectors · Modal time history load case · Direct integration time history load case · Ramp loading 	Hand calculation using theory presented in section 4.5 on Pages 126 through 129 of Chopra 1995.
6-002	Multi-linear Elastic Link	<ul style="list-style-type: none"> · Multi-linear links · Displacement-controlled nonlinear static analysis 	Comparison with defined link force- deformation characteristics.
6-003	Gap Element	<ul style="list-style-type: none"> · Gap element links · Force-controlled nonlinear static analysis · Nonlinear modal time history analysis · Nonlinear direct time history analysis · Frame point loads · Joint force loads · Joint mass assignments · Ramp loading for time histories 	Hand calculation using the unit load method described on page 244 in Cook and Young 1985.
6-004	Hook Element	<ul style="list-style-type: none"> · Hook element links · Force-controlled nonlinear static analysis · Frame temperature loads 	Hand calculation using standard thermal expansion formulas.
6-005	Damper Element Under Harmonic Loading	<ul style="list-style-type: none"> · Damper element links · Linear link elements · Nonlinear modal time history analysis · Nonlinear direct integration time history analysis · Joint force loads 	Hand calculation using equation 3.2.6 on page 7 in Chopra 1995.

6-006	SUNY Buffalo Damper with Linear Velocity Exponent	<ul style="list-style-type: none"> · Damper links with linear velocity exponents · Frame end length offsets · Joint mass assignments · Modal analysis for Ritz vectors · Linear modal time history analysis · Nonlinear modal time history analysis · Linear direct integration time history analysis · Nonlinear direct integration time history analysis · Generalized displacements 	Comparison with experimental results from shake table tests published in Section 5, pages 61 through 73, of Scheller and Constantinou 1999.
6-007	SUNY Buffalo Damper with Nonlinear Velocity Exponent	<ul style="list-style-type: none"> · Damper links with nonlinear velocity exponents · Frame end length offsets · Joint mass assignments · Modal analysis for Ritz vectors · Nonlinear modal time history analysis · Nonlinear direct integration time history analysis · Generalized displacements 	Comparison with experimental results from shake table tests published in Section 5, pages 61 through 73, of Scheller and Constantinou 1999.
6-008	Plastic Wen Link	<ul style="list-style-type: none"> · Plastic Wen links · Displacement-controlled nonlinear static analysis · Link local axis assignments · Link gravity load 	Comparison with defined link force- deformation characteristics.
6-009	Plastic Kinematic Link	<ul style="list-style-type: none"> · Plastic kinematic links · Displacement-controlled nonlinear static analysis · Link gravity load 	Comparison with defined link force- deformation characteristics.
6-010	SUNY Buffalo Eight-Story Building with Rubber Isolators	<ul style="list-style-type: none"> · Rubber isolator links · Linear links · Zero-length, two-joint link elements · Diaphragm constraints · Modal analysis for Ritz vectors · Nonlinear modal time history analysis · Nonlinear direct integration time history analysis · Generalized displacements 	Comparison with results from the computer program 3D-BASIS-ME (see Tsopelas, Constantinou and Reinhorn 1994) published in Section 2, pages 5 through 23, of Scheller and Constantinou 1999.

6-011	SUNY Buffalo Seven-Story Building with Friction Pendulum Isolators	<ul style="list-style-type: none"> · Friction pendulum link elements · Damper link elements · Zero-length, two-joint link elements · Diaphragm constraints · Frame end length offsets · Modal analysis for Ritz vectors · Nonlinear modal time history analysis · Nonlinear direct integration time history analysis · Joint masses 	Comparison with experimental results from shake table tests published in Section 4, pages 43 through 59, of Scheller and Constantinou 1999.
6-012	Frequency-Dependent Links	<ul style="list-style-type: none"> · Frequency-dependent links · Steady state analysis 	Hand calculation using formulas and theory presented in section 3.2 on pages 68 through 69 of Chopra 1995.

Table 8: SASSI2010 Verification Problem No. 1 Analysis Cases

SASSI Case No.		Element Type Verified	SASSI Model Description	Method of Forming Impedance	Excitation
1	(a)	3D Brick	Determine horizontal and rocking impedance of a rigid massless circular foundation.	Direct (Flexible Volume)	Horizontal and rocking harmonic force excitation.
	(b)	3D Brick, 3D Beam	Determine SSI response of a surface founded pressurized water reactor (PWR) containment building.	Direct (Flexible Volume)	Horizontal ground motion excitation prescribed in the form of vertically propagating SV wave.

Table 9: SASSI2010 Verification Problem No. 2 Analysis Cases

SASSI Case No.	Element Type Verified	SASSI Model Description	Method of Forming Impedance	Excitation
1	(a)	3D Brick Scattering response of embedded rigid cylinder, $H=0.5$, uniform soil profile.	<ul style="list-style-type: none"> · Direct · Extended Subtraction · Subtraction 	Horizontal ground motion excitation prescribed in the form of horizontally propagating SH wave.
	(b)	Same as Case 1(a) Same as Case 1(a).		Horizontal ground motion excitation prescribed in the form of vertically propagating SV wave.
2	(a)	3D Brick Scattering response of embedded rigid cylinder, $H=1.0$, uniform soil profile.	<ul style="list-style-type: none"> · Direct · Extended Subtraction · Subtraction 	Horizontal ground motion excitation prescribed in the form of horizontally propagating SH wave.
	(b)	Same as Case 2(a) Same as Case 2(a).		Horizontal ground motion excitation prescribed in the form of vertically propagating SV wave.
3	(a)	3D Brick Scattering response of embedded rigid cylinder, $H=2.0$, uniform soil profile.	<ul style="list-style-type: none"> · Direct · Extended Subtraction · Subtraction 	Horizontal ground motion excitation prescribed in the form of horizontally propagating SH wave.
	(b)	Same as Case 3(a) Same as Case 3(a).		Horizontal ground motion excitation prescribed in the form of vertically propagating SV wave.
4	-	3D Brick Scattering response of embedded rigid cylinder, $H=1.0$, inverted soil profile.	<ul style="list-style-type: none"> · Direct · Extended Subtraction · Subtraction 	Horizontal ground motion excitation prescribed in the form of vertically propagating SV wave.
5	-	3D Brick Scattering response of embedded rigid cylinder, $H=2.0$, inverted soil profile.	<ul style="list-style-type: none"> · Direct · Extended Subtraction · Subtraction 	Horizontal ground motion excitation prescribed in the form of vertically propagating SV wave.
6	-	3D Brick Scattering response of embedded rigid cylinder, $H=1.0$, increasing soil profile.	<ul style="list-style-type: none"> · Direct · Extended Subtraction · Subtraction 	Horizontal ground motion excitation prescribed in the form of vertically propagating SV wave.
7	-	3D Brick Scattering response of embedded rigid cylinder, $H=2.0$, increasing soil profile.	<ul style="list-style-type: none"> · Direct · Extended Subtraction · Subtraction 	Horizontal ground motion excitation prescribed in the form of vertically propagating SV wave.

Table 10: SASSI2010 Verification Problem No. 3 Analysis Cases

SASSI Case No.	Element Type Verified	SASSI Model Description	Method of Forming Impedance	Excitation
1	3D Brick, 3D Plate/Shell, 3D Beam	SSI Response of Lotung 1/4 Scale Containment Model.	<ul style="list-style-type: none"> · Direct (Flexible Volume) · Extended Subtraction · Subtraction 	Horizontal ground motion excitation prescribed in the form of vertically propagating SV wave.

Table 11: SASSI2010 Verification Problem No. 4 Analysis Cases

SASSI Case No.	Element Type Verified	SASSI Model Description	Method of Forming Impedance	Excitation
1	3D Brick, 3D Inter-Pile, 3D Beam	Horizontal and vertical response at the pile head of a single pile in a homogeneous halfspace using inter-pile elements.	Subtraction	Horizontal and vertical harmonic loading applied at center of pilecap.
2	3D Brick, 3D Inter-Pile, 3D Beam	Horizontal and vertical response at the pile head of a 2×2 pile group with S/D=2 in a homogeneous halfspace using inter-pile elements.	Subtraction	Horizontal and vertical harmonic loading applied at center of pilecap.
3	3D Brick, 3D Inter-Pile, 3D Beam	Horizontal and vertical response at the pile head of a 2×2 pile group with S/D=5 in a homogeneous halfspace using inter-pile elements.	Subtraction	Horizontal and vertical harmonic loading applied at center of pilecap.
4	3D Brick, 3D Inter-Pile, 3D Beam	Horizontal and vertical response at the pile head of a 3×3 pile group with S/D=2 in a homogeneous halfspace using inter-pile elements.	Subtraction	Horizontal and vertical harmonic loading applied at center of pilecap.

Table 12: SASSI2010 Verification Problem No. 5 Analysis Cases

SASSI Problem 5 Case No.	Element Type Verified	SASSI Model Description	Method of Forming Impedance	Excitation
1	3D Brick, 3D Beam	Horizontal and vertical response at the pile head of 2×2 pile groups with S/D=2, 5, and 10 in a homogeneous halfspace using the pile impedance method.	Direct	Horizontal and vertical harmonic loading applied at center of pilecap.
2	3D Brick, 3D Beam	Horizontal and vertical response at the pile head of 3×3 pile groups with S/D=2, 5, and 10 in a homogeneous halfspace using the pile impedance method.	Direct	Horizontal and vertical harmonic loading applied at center of pilecap.
3	3D Brick, 3D Beam	Horizontal and vertical response at the pile head of 4×4 pile groups with S/D=2, 5, and 10 in a homogeneous halfspace using the pile impedance method.	Direct	Horizontal and vertical harmonic loading applied at center of pilecap.

Table 13: SASSI2010 Verification Problem No. 6 Analysis Cases

SASSI Problem 6 Case No.	Element Type Verified	SASSI Model Description	Method of Forming Impedance	Excitation
1	3D Thick Shell, 3D Beam	Determine SSI response of a surface-founded pressurized water reactor (PWR) containment building.	Direct	Horizontal ground motion excitation prescribed in the form of horizontally propagating SV wave. Coherent ground motion (30 time histories)
2	3D Thick Shell, 3D Beam	Determine SSI response of a surface-founded pressurized water reactor (PWR) containment building.	Direct	Horizontal ground motion excitation prescribed in the form of horizontally propagating SV wave. Coherent ground motion (Random Vibration Theory)
3	3D Thick Shell, 3D Beam	Determine SSI response of a surface-founded pressurized water reactor (PWR) containment building.	Direct	Horizontal ground motion excitation prescribed in the form of horizontally propagating SV wave. Incoherent ground motion (30 time histories)
4	3D Thick Shell, 3D Beam	Determine SSI response of a surface-founded pressurized water reactor (PWR) containment building.	Direct	Horizontal ground motion excitation prescribed in the form of horizontally propagating SV wave. Incoherent ground motion (Random Vibration Theory)

Table 14: SASSI2010 Verification Problem No. 7 Analysis Cases

SASSI Problem 7 Case No.	Element Type Verified	SASSI Model Description	Excitation
1	(a) Rectangular Brick	Two elements form a column of 1'x1' in cross section and 4' in height supported on the surface of a rigid halfspace.	Vertical harmonic force excitation
	(b) Triangular Brick	Four elements form the same column as in Case 1(a)	Vertical harmonic force excitation
2	(a) 3D Beam	Five elements were used to form a cantilever beam supported on the surface of a rigid halfspace.	Harmonic lateral force excitations applied at the tip of the beam.
	(b) 3D Beam	Same as Case 2(a)	Horizontal ground motion excitation prescribed in the form of vertically propagating SV wave.
	(c) 3D Beam	Same as Case 2(a). Test COMBIN module.	Same as Case 2(b)
3	(a) 3D Plate/Shell	A 100'x100' x10' vertical square plate supported on horizontal plate of the same size supported on a rigid halfspace.	Out-of-plane horizontal harmonic line-load excitations
	(b) same as 3(a)	Same as 3(a) except thickness=20'	In-plane horizontal harmonic line-load excitation
4	(a) 2D Plane Strain	Two elements form a vertical wall of a unit width supported on the surface of a rigid halfspace.	Harmonic axial load excitation applied at top of the wall
	(b) 2D Plane Strain	Same as Case 4(a). Test COMBIN module.	Same as Case 4(a)
5	- 3D Spring	Two elements form two single-degree-of-freedom (SDOF) systems supported on the surface of a rigid halfspace.	Vertical harmonic force excitations
6	- 3D Generalized Stiffness/Mass Matrix	(Same as for 3D Springs)	Vertical harmonic force excitations
7	- 3D Thick Shell Element	A 100'x100' x10' vertical square plate supported on horizontal plate of the same size supported on a rigid halfspace.	Horizontal and vertical harmonic line-load excitations

Table 15: SASSI2010 Verification Problem No. 8 Analysis Cases

SASSI Problem 8 Case No.		Element Type Verified	SASSI Model Description	Excitation
1	(a)	2D Plane Strain	A rigid massless strip foundation on the surface of a uniform viscoelastic soil overlaying rigid rock. The strip foundation was modeled in 2D using a one-half model consisting of 5 plane-strain elements and 12 node points.	Vertical harmonic force excitation
	(b)	3D Plate/Shell	A rigid massless strip foundation on the surface of a uniform viscoelastic soil overlaying rigid rock. The strip foundation was modeled in 3D as an elongated rectangular foundation using a one-quarter model consisting of 250 3D flat plate/shell elements and 306 node points.	Vertical harmonic force excitation

Table 16: SASSI2010 Verification Problem No. 9 Analysis Cases

SASSI Problem 9 Case No.	Element Type Verified	Model Description	Excitation
1	3D Brick, 3D Beam	A rigid circular disk resting on a uniform elastic half space subjected to seismic ground motion including the effects of incoherency.	<ul style="list-style-type: none"> · Horizontal ground motion excitation prescribed in the form of vertically propagating SV wave. · Vertical ground motion excitation prescribed in the form of vertically propagating P wave.

Table 17: SASSI2010 Verification Problem No. 10 Analysis Cases

SASSI Problem 10 Case No.	Element Type Verified	Model Description	Methods and Results of Verification										
1	Brick, Beam, Shell, Link	<div><div>A surface-founded, fixed-base nuclear reactor building SASSI model described in Reference 14 of ER-F010-6084, Rev. 0. The model has a total weight of 859,078 kips and consists of:</div><table><tr><td>32,378</td><td>nodes</td></tr><tr><td>12,075</td><td>solid elements</td></tr><tr><td>6,453</td><td>beam elements</td></tr><tr><td>18,818</td><td>shell (plate) elements</td></tr><tr><td>3,306</td><td>link (spring) elements</td></tr></table></div>	32,378	nodes	12,075	solid elements	6,453	beam elements	18,818	shell (plate) elements	3,306	link (spring) elements	<div><div>· Comparing total base reactions due to gravity in the three global directions calculated by SASSI2010 with those verified by SAP2000. The differences in reactions are less than 0.00015%.</div><div>· Comparing the structural frequencies calculated by SASSI2010 with those by verified SAP2000. The major structural frequencies obtained at the amplification peaks in the transfer functions calculated by SASSI2010 are compared with the corresponding modal frequencies by SAP2000. The differences in structural frequencies between SASSI2010 and SAP2000 are less than 8%. The frequency differences are deemed acceptable. The differences can be attributed mostly to</div><div>a. SASSI2010 cannot completely simulate the fixed-base condition by seating the reactor building on a very stiff free-field half space.</div><div>b. Different methods in assigning material damping between SASSI2010 (complex damping) and SAP2000 (Rayleigh damping).</div><div>c. Two different numerical solution procedures between SASSI2010 (frequency domain) and SAP2000 (time domain).</div></div>
32,378	nodes												
12,075	solid elements												
6,453	beam elements												
18,818	shell (plate) elements												
3,306	link (spring) elements												

2	Brick, Beam, Shell, Link	<p>A surface-founded, fixed-base nuclear control building SASSI model.</p> <p>The model has a total weight of 127,750 kips and consists of:</p> <table><tr><td>9,279</td><td>nodes</td></tr><tr><td>3,966</td><td>solid elements</td></tr><tr><td>1,393</td><td>beam elements</td></tr><tr><td>4,069</td><td>shell (plate) elements</td></tr><tr><td>864</td><td>link (spring) elements</td></tr></table>	9,279	nodes	3,966	solid elements	1,393	beam elements	4,069	shell (plate) elements	864	link (spring) elements	<ul style="list-style-type: none">· Comparing total base reactions due to gravity in the three global directions calculated by SASSI2010 with those verified by SAP2000. The differences in reactions are less than 0.0025%.· Comparing the structural frequencies calculated by SASSI2010 with those by verified SAP2000. <p>The major structural frequencies obtained at the amplification peaks in the transfer functions calculated by SASSI2010 are compared with the corresponding modal frequencies by SAP2000. The differences in structural frequencies between SASSI2010 and SAP2000 are less than 4%. The frequency differences are deemed acceptable. The differences can be attributed mostly to</p> <ul style="list-style-type: none">a. SASSI2010 cannot completely simulate the fixed-base condition by seating the reactor building on a very stiff free-field half space.b. Different methods in assigning material damping between SASSI2010 (complex damping) and SAP2000 (Rayleigh damping).c. Two different numerical solution procedures between SASSI2010 (frequency domain) and SAP2000 (time domain).
9,279	nodes												
3,966	solid elements												
1,393	beam elements												
4,069	shell (plate) elements												
864	link (spring) elements												

Table 18: SHAKE2000 Verification Problems

SHAKE2000 Problem No.	SHAKE2000 Verification Problem Description	Excitation Input	SHAKE2000 Capabilities to be Verified	Methodology
1	Uniform undamped elastic half space subjected to a harmonic ground motion at the soil surface, i.e., free-field input motion	Free-field horizontal harmonic acceleration	<ul style="list-style-type: none"> · Amplification Spectrum, i.e., ratio of acceleration amplitudes between any two layers. · Shear strain/stress time history response calculation · Calculation of maximum shear strain/stress vs. depth · Calculation of maximum acceleration vs. depth 	Closed-form solution
2	Two-layered soil subjected to a harmonic ground motion at the soil surface, i.e., free-field input motion	Free-field horizontal harmonic acceleration	<ul style="list-style-type: none"> · Amplification Spectrum at any typical layer · Amplification vs. depth 	Closed-form solution
3	Multi-layered soil subjected to a harmonic ground motion at the bedrock.	Harmonic horizontal excitation at top of bedrock	Amplification Spectrum	Closed-form solution
4	Multi-layered soil subjected to a seismic ground motion at the Ground Surface.	Horizontal seismic excitation at Ground Surface	<ul style="list-style-type: none"> · Amplification Spectrum · Calculation of transient acceleration response time history 	Results calculated by a validated SHAKE Program

5	Multi-layered soil subjected to a seismic ground motion at the bedrock.	Horizontal seismic excitation at top of bedrock	<ul style="list-style-type: none"> · Calculation of strain-compatible soil shear modulus and damping ratios for soil layers through iteration · Calculation of acceleration response spectrum of acceleration response time history of any soil layer 	<ul style="list-style-type: none"> · Manual iteration · Response Spectrum calculated by the validated SAP2000 Program
6	Uniform undamped elastic half -space modeled by 200 soil layers subjected to a harmonic ground motion at the soil surface, i.e., free-field input motion	Free-field horizontal sinusoidal acceleration	Verify the limitation on the maximum number of layers of 200.	Closed-form solution

Table 19: RSPMATCH Verification Problems

RspMatchEDT Test Case No.	RspMatch2009 Capability to Verify	Methodology
1	Modify a seed acceleration time history so that the response spectrum of the modified time history closely resembles a target spectrum.	The target spectrum used is from an ARES calculation. The seed acceleration time history used is from published data of an actual recorded earthquake.
2	Accurately generate a response spectrum.	The response spectrum calculated by the program for an arbitrary selected acceleration time history is compared with one calculated by the validated program SAP2000.

Impact on DCA:

FSAR Tier 2, Section 3.7.5 has been revised as described in the response above and as shown in the markup provided in this response.

3.7.5 Computer Programs Used in Section 3.7 Seismic Design

Only commercially available software packages were used for the analysis and design of the site-independent Seismic Category I and Seismic Category II structures. The primary software packages used are SAP2000 and SASSI2010.

RAI 03.07.02-7

The software validation and verification summary tests those characteristics of the software that mimic the physical conditions, material properties, and physical processes that represent the NuScale design in numerical analysis. It covers the full range of parameters used in NuScale design-basis seismic demand calculations including the discretization and aspect ratio of finite elements, Poisson's ratio, frequencies of analysis, and other parameters pertinent to seismic system analyses.

3.7.5.1 ANSYS

3.7.5.1.1 Description

RAI 03.07.02-7

ANSYS is a commercial, general use finite element analysis (FEA) software. ANSYS is used to determine demand loads and stresses in structures, supports, equipment, and components/assemblies. ANSYS Mechanical software offers a comprehensive product solution for structural linear and nonlinear and dynamic analysis. The product provides a complete set of element behavior, material models, and equation solvers for a wide range of engineering problems.~~ANSYS is a finite element program for a broad range of structural and mechanical analyses.~~

3.7.5.1.2 Version Used

ANSYS Computer Program, Release 14, 15, and 16.0, January 2015. ANSYS Incorporated, Canonsburg, Pennsylvania.

RAI 03.07.02-7

3.7.5.1.3 Validation and Verification

RAI 03.07.02-7

Software validation and verification was performed in accordance with the NuScale Quality Assurance program. This included confirmation that the software was capable of addressing the NuScale design conditions and performance of the ~~ANSYS~~-provided verification testing package.

3.7.5.1.4 Extent of Use

ANSYS is used for fluid structure interaction applying input motions from SASSI2010 and using fluid elements to assess the fluid pressures on walls and sloshing heights. Factors are applied to SASSI2010 results to adjust for these effects.

3.7.5.2 SAP2000**3.7.5.2.1 Description**

RAI 03.07.02-7

SAP2000 is a general-purpose, three-dimensional, static and dynamic finite-element computer program. Analyses, including calculation of deflections, forces, and stresses, may be done on structures constructed of any material or combination of materials.

RAI 03.07.02-7

It features a powerful graphical interface which is used to create/modify finite element models. This same interface is used to execute the analysis and for checking the optimization of the design. Graphical displays of results, including real-time animations of time-history displacements, are produced. SAP2000 provides automated generation of loads for design based on a number of National Standards.

RAI 03.07.02-7

The software can perform the following types of analyses: static linear analysis, static nonlinear analysis, modal analysis, dynamic response spectrum analysis, dynamic linear and nonlinear time history analysis, bridge analysis, moving load analysis, and buckling analysis. ~~SAP2000 is a finite element program for analysis and design of structures. It performs both static and dynamic analysis.~~

3.7.5.2.2 Version Used

SAP2000, Version 18.1.1, Computers and Structures, Inc., Berkeley.

RAI 03.07.02-7

3.7.5.2.3 Validation and Verification

Software validation and verification was performed in accordance with NuScale Quality Assurance program. This included confirmation that the software was capable of addressing the NuScale design conditions and performance of the Computer and Structures Inc. verification problems.

3.7.5.2.4 Extent of Use

SAP2000 is used to develop the finite element models of the RXB and CRB and to perform general structural analysis of the building.

3.7.5.3 SASSI2010**3.7.5.3.1 Description**

RAI 03.07.02-7

SASSI, a System for Analysis of Soil-Structure Interaction, consists of a number of interrelated computer program modules which can be used to solve a wide range of dynamic soil-structure interaction (SSI) problems in two or three dimensions.~~SASSI2010 is used to solve a wide range of dynamic soil-structure interaction (SSI) problems, including layered soil conditions and embedment conditions, in two or three dimensions.~~

3.7.5.3.2 Version Used

SASSI2010 Version 1.0, Berkeley, California

RAI 03.07.02-7

3.7.5.3.3 Validation and Verification

RAI 03.07.02-7

Software validation and verification was performed in accordance with NuScale Quality Assurance program. This included confirmation that ~~SSASS2010~~SASSI2010 was capable of analyzing a model as large and complex as planned for the RXB, the CRB, and the RWB, and capable of using the earthquake profiles with the accelerations and frequency range of the CSDRS and CSDRS-HF. In addition, test problems were evaluated to confirm the adequacy of the program.

3.7.5.3.4 Extent of Use

SASSI2010 is used to obtain seismic design loads and in-structure floor response spectra for the Seismic Category I buildings accounting for the effects of SSI.

3.7.5.4 SHAKE2000

3.7.5.4.1 Description

RAI 03.07.02-7

The computer program SHAKE2000 computes the free-field response of a semi-infinite, horizontally layered soil column overlying a uniform half-space subjected to an input motion prescribed as the object motion in the form of vertically propagating shear waves. SHAKE2000 is used for the analysis of site-specific response and for the evaluation of earthquake effects on soil deposits. It provides an approximation of the dynamic response of a site. SHAKE2000 computes the response in a system of homogeneous, viscoelastic layers of infinite horizontal extent subjected to vertically traveling shear waves.~~SHAKE2000 is used to perform the free-field site response analysis to generate the design earthquake-induced strain-compatible free-field soil properties and site response motions required in the seismic SSI analysis.~~

3.7.5.4.2 Version Used

SHAKE2000, a module of GeoMotions Suite, Version 9.98.0, Gustavo A. Ordonez.

RAI 03.07.02-7

3.7.5.4.3 Validation and Verification

RAI 03.07.02-7

Software validation and verification was performed in accordance with [the](#) NuScale Quality Assurance program. Sample problems were designed to test SHAKE2000 major analytical capabilities.

3.7.5.4.4 Extent of Use

RAI 03.07.02-7

SHAKE2000 is used to generate strain-compatible soil properties and free-field site response motions for use in seismic SSI analysis of the site-independent Seismic Category I and Seismic Category II structures.

3.7.5.5 RspMatch2009**3.7.5.5.1 Description**

RAI 03.07.02-7

RspMatch2009 is used to generate spectrum-compatible acceleration time histories by modifying a recorded seismic accelerogram. [The RspMatch2009 program performs a time domain modification of an acceleration time history to make it compatible with a user-specified target spectrum.](#)

3.7.5.5.2 Version Used

RspMatch2009, Version 2009

RAI 03.07.02-7

3.7.5.5.3 Validation and Verification

RAI 03.07.02-7

Software validation and verification was performed in accordance with [the](#) NuScale Quality Assurance program. The program was validated by comparing the response spectrum calculated by RspMatch 2009 for an arbitrarily selected acceleration time history with one calculated by SAP2000 for the same acceleration time history.

3.7.5.5.4 Extent of Use

RAI 03.07.02-7

RspMatch2009 is used to generate the five CSDRS-compatible acceleration time histories by modifying the recorded seismic accelerograms of five different

earthquakes and to generate the CSDRS-HF-compatible acceleration time history by modifying the recording of the time histories of a sixth earthquake.

3.7.5.6 RspMatchEDT

3.7.5.6.1 Description

RAI 03.07.02-7

RspMatchEDT is used to generate spectrum-compatible acceleration time histories by modifying a recorded seismic accelerogram. [The RspMatchEDT Module for SHAKE2000 is a pre- and post-processor for the RspMatch2009 program, which is part of SHAKE2000.](#)

3.7.5.6.2 Version Used

RspMatchEDT, a module of GeoMotions Suite, Version 9.98.0, Gustavo A. Ordonez.

RAI 03.07.02-7

3.7.5.6.3 Validation and Verification

RAI 03.07.02-7

Software validation and verification was performed in accordance with [the](#) NuScale Quality Assurance program. The program was validated by comparing the response spectrum calculated by RspMatchEDT with the spectrum calculated by RspMatch2009.

3.7.5.6.4 Extent of Use

RspMatchEDT is used to confirm the adequacy of the CSDRS and CSDRS-HF compatible time histories produced with RspMatch2009.